AD-A190 256 COMPARISON OF ENTROPY GENERATION AND CONVENTIONAL DESIGN METHODS FOR HEAT EXCHANGERS(U) MASSACHUSETTS INST OF TECH CAMBRIDGE DEPT OF OCEAN ENGINEERIN 1/1

UNCLASSIFIED D S HERBEIN JUN 87 N00228-85-G-3262 F/G 13/10 NL

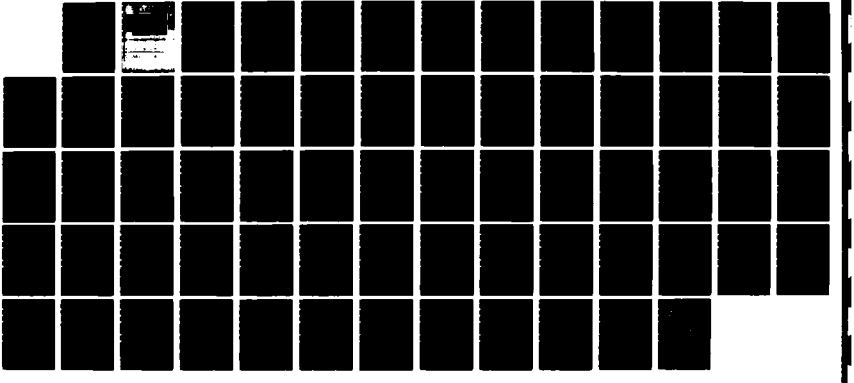

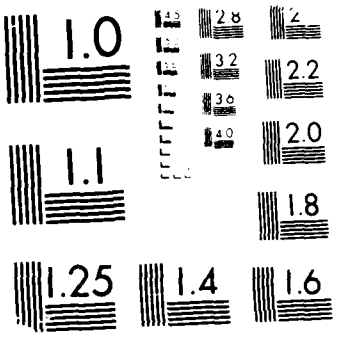

MICROCOPY RESOLUTION TEST CHART

AD-A190 256

DEPARTMENT OF OCEAN ENGINEERING
MASSACHUSETTS INSTITUTE OF TECHNOLOGY
CAMBRIDGE, MASSACHUSETTS 02139

DTIC FILE COPY
JAN 20 1988

COMPARISON OF ENTROPY GENERATION AND CONVENTIONAL DESIGN METHODS FOR HEAT EXCHANGERS

by

David Samuel Herbein

DISTRIBUTION STATEMENT A
Approved for public release;
Distribution Unlimited

XIII-A

June 1987

N00228-85-G-3262

COMPARISON OF ENTROPY GENERATION AND CONVENTIONAL DESIGN METHODS FOR HEAT EXCHANGERS

by

David Samuel Herbein
B.S. Marine Engineering
United States Naval Academy
(1975)

Submitted to the Department of Ocean Engineering
in Partial Fulfillment of the Requirements for the
Degrees of
NAVAL ENGINEER
and
MASTER OF SCIENCE IN NAVAL ARCHITECTURE AND
MARINE ENGINEERING
at the
MASSACHUSETTS INSTITUTE OF TECHNOLOGY
June, 1987

©David Samuel Herbein, 1987

The author hereby grants to M.I.T. and to the U.S. Government permission to reproduce and to distribute copies of this thesis document in whole or in part.

Signature of Author David S. Herbein
Department of Ocean Engineering
May 8, 1987

Certified by Warren M. Rohsenow
Warren M. Rohsenow
Thesis Supervisor

Approved by Clark Graham
Clark Graham
Thesis Reader

Accepted by A. Douglas Carmichael
A. Douglas Carmichael
Chairman, Ocean Engineering Departmental Committee

DTIC
ELECTE
JAN 20 1988
H

DISTRIBUTION STATEMENT A
Approved for public release;
Distribution Unlimited

38 1 ? 037

COMPARISON OF ENTROPY GENERATION AND CONVENTIONAL DESIGN METHODS FOR HEAT EXCHANGERS

by

David Samuel Herbein

Submitted to the Ocean Engineering Department on May 8, 1987 in partial fulfillment of the requirements for the degrees of Naval Engineer and Master of Science in Naval Architecture and Marine Engineering.

Abstract

The design of heat exchangers traditionally focuses on the known constraints of the problem such as inlet and outlet temperatures, flow rates, and pressure drops. This leads mainly to a sizing problem where the designer must select surfaces, flow configuration, and materials to meet the minimum design objectives. An alternate approach based on an acceptable level of thermodynamic irreversibility (entropy generation) has been proposed. When the entropy generation level has been set, the geometric parameters of the heat exchanger can be determined. The design of a plate-fin type, gas-to-gas recuperator for a regenerative open Brayton cycle has been used as a demonstrative device. The resulting heat exchanger designs are then examined to determine what caused the differences and why either method should be preferred over the other.

Thesis Supervisor: Dr. Warren M. Rohsenow

Title: Professor of Mechanical Engineering

A-1

Acknowledgements

The author wishes to extend his sincere gratitude to Professor Warren M. Rohsenow for his kind support and guidance during the preparation of this thesis. His willingness to invest his time and effort in this undertaking is greatly appreciated.

A special thanks to Denise Cormier for turning pages of handwritten dribble into the clear, easy to read text you see before you.

The author wishes to acknowledge one of America's corporate giants, the Hewlett–Packard Corporation. All calculations performed in support of this thesis were accomplished on their sturdy, robust HP-11C calculator without a single failure.

Finally, the author is most grateful to the four girls in his life for providing enough diversions to avoid his non-dimensionalization, but not too many as to hinder his progress. Their support and patience throughout the preparation of this thesis were greatly appreciated.

Contents

1 INTRODUCTION 10

1.1 Background 10

1.2 Conventional Design Procedures 10

1.3 Irreversibility Minimization 11

2 SELECTION OF BRAYTON CYCLE PARAMETERS 12

2.1 Cycle Components 12

2.2 Cycle Parameters 13

2.3 Heat Exchanger Characteristics 14

3 CONVENTIONAL DESIGN METHOD 15

3.1 Introduction 15

3.2 Conventional Methodology 15

3.3 Analysis 16

4 MINIMUM ENTROPY DESIGN METHOD 19

4.1 Introduction 19

4.2 Background 19

4.3 Design Considerations 22

4.4 Minimum Entropy Design Methodology 23

4.5 Analysis 24

5 COMPARISONS AND RESULTS 27

5.1 Introduction 27

5.2 Conventional Method Entropy Generation 27

5.3 Minimum Entropy Generation 28
5.4 Comparisons 28

6 CONCLUSIONS **39**
6.1 Discussion 39
6.2 Conclusions 39

A Sample Calculation for Effect of Recuperator on Cycle Efficiency **40**

B Conventional Design Method Numerical Example **42**
B.1 Temperatures and Fluid Properties 44
B.2 N_{tu} 46
B.3 Estimated Pressure Drops 46
B.4 Mass Velocities 47
B.5 Heat Transfer Coefficients and Fin Effectivenesses 48
B.6 Dimensions 50
B.7 Calculated Pressure Drops 51

C Minimum Entropy Design Method Numerical Example **53**
C.1 Optimum Length 53
C.2 Heat Exchanger Effectiveness and Pressure Drops 54
C.3 Entropy Generation 55
C.4 Heat Exchanger Volume 55
C.5 Cycle Efficiency Degrade 55

D Sample Calculation of Entropy Generation for Conventional Designs **57**

List of Figures

Figure		Page
2.1	Regenerative Cycle Schematic	12
2.2	Cycle Efficiency vs. Pressure Ratio	13
2.3	Plain Plate-Fin Surface 2.0	14
3.1	Efficiency Degrade vs. Effectiveness	19
3.2	Volume vs. Effectiveness	20
3.3	Volumes at Constant Cycle Degrade	21
3.4	"Minimum" Volume vs. Effectiveness	22
4.1	Recuperator Control Volume	24
4.2	Efficiency Degrade vs. Minimum Entropy Effectiveness	30
4.3	Minimum Entropy Volume vs. Effectiveness	31
5.1	Cycle Efficiency Degrade vs. Entropy Generated	36
5.2	"Minimum" Volume vs. Entropy Generated	37
5.3	Cycle Efficiency Degrade vs. Minimum Entropy Generated	38
5.4	"Optimum" Volume vs. Minimum Entropy Generated	39
5.5	Volume vs. Entropy Comparison	40
5.6	Case E-9 (L/r_h) Optimization	41
5.7	Volumes along Constant G Path	42
5.8	Volume vs. Cycle Efficiency Degrade Comparison	43
B.1	Temperature-Entropy Diagram	48

List of Tables

3.1 Conventional Method Results 18

4.1 Entropy Generation Method Results 29

5.1 Conventional Method Entropy Generation 35

List of Symbols

a	imbalance coefficient
A	heat transfer surface area
A_f	fin area
A_{fr}	frontal area
A_o	minimum free flow area
b	imbalance coefficient
B	ideal gas constants ratio
c_p	specific heat at constant pressure
C	capacity rate
C^*	capacity ratio, C_{min}/C_{max}
d	plate spacing
D_h	hydraulic diameter
f	friction factor
g	dimensionless mass velocity
G	mass velocity
h	heat transfer coefficient
$\dot{I}$	rate of thermodynamic irreversibility
j	Colburn factor
k	summation of hot and cold pressure losses
k_f	thermal conductivity of fin material
l	fin length
L	flow length
m	fin characteristic length
$\dot{m}$	mass flow rate
N_{Pr}	Prandtl number
N_{Re}	Reynolds number
N_s	number of entropy generation units
$N_{s,\Delta P}$	N_s due to friction ΔP in the channel
$N_{s,\Delta T}$	N_s due to heat transfer across a finite ΔT
N_{St}	Stanton number
N_{tu}	number of heat transfer units
P	pressure, absolute

$\dot{Q}$	combustor heat input
r	pressure ratio, P_h/P_c
r_h	hydraulic radius
R	ideal gas constant
s	specific entropy
$\dot{S}$	rate of entropy production
t	parting plate thickness
T	temperature, absolute
U	overall heat transfer coefficient
Vol	heat exchanger volume
$\dot{w}$	mechanical power
$\dot{w}_c$	compressor work
$\dot{w}_t$	turbine work
α	ratio of heat transfer area to total volume
β	surface area density
δ	fin thickness
Δ	difference
ϵ	heat exchanger effectiveness
γ	ratio of specific heats, c_p/c_v
η	cycle efficiency with losses
η_∞	cycle efficiency without losses
η_f	temperature effectiveness of fin
η_0	total surface temperature effectiveness
η_{pc}	polytropic compressor efficiency
η_{pt}	polytropic turbine efficiency
ρ	gas density
$(1/\rho)_m$	mean specific volume
σ	ratio of A_0/A_{fr}
τ	temperature span parameter
θ	non-dimensional mean temperature ratio
μ	dynamic viscosity

Chapter 1

INTRODUCTION

1.1 Background

Energy conservation is a topic that has recently received considerable attention. Available work has been recognized as a valuable commodity and its destruction in seemingly otherwise efficient engineering processes has also seen a renewed increase in interest. The use of second law analysis and thermodynamic irreversibility minimization have been proposed as techniques that should become an integral part of the design of engineering processes and components [1]. It is not apparent what the relationship of traditional methods of design and these irreversibility minimization techniques will be.

1.2 Conventional Design Procedures

The design of a component, such as a heat exchanger, generally involves the sizing of that component to meet specified performance parameters within known constraints. The heat exchanger area and volume are usually designed to be the minimum required to meet the specifications as this will also usually be the best design from an ecomonic aspect. The fluid inlet and outlet temperatures, flow rates, and pressure drops are usually specified and it is the designer's task to determine construction type, flow arrangement, materials and surfaces to meet those requirements [2]. The effect of the component design on the overall system performance should also be consid-

ered to ensure the tradeoffs performed within its design are still valid when integrated into the system.

1.3 Irreversibility Minimization

Any heat transfer process is generally accompanied by thermodynamic irreversibility or entropy generation. The entropy generated is in direct proportion to the amount of useful work dissipated in that process. If this irreversibility can be minimized within a particular component of a power cycle, the useful power output of the cycle should increase [3]. Bejan has shown how the entropy generation rate can be reduced in a counterflow gas-to-gas heat exchanger [4], and it is this method that will be used to create designs that will be compared to conventionally designed heat exchangers, and their impact on overall cycle performance.

Chapter 2

SELECTION OF BRAYTON CYCLE PARAMETERS

2.1 Cycle Components

A regenerative open Brayton cycle was chosen as the vehicle to test the different design methods for the recuperator. A schematic of the cycle components is shown in Figure 2.1.

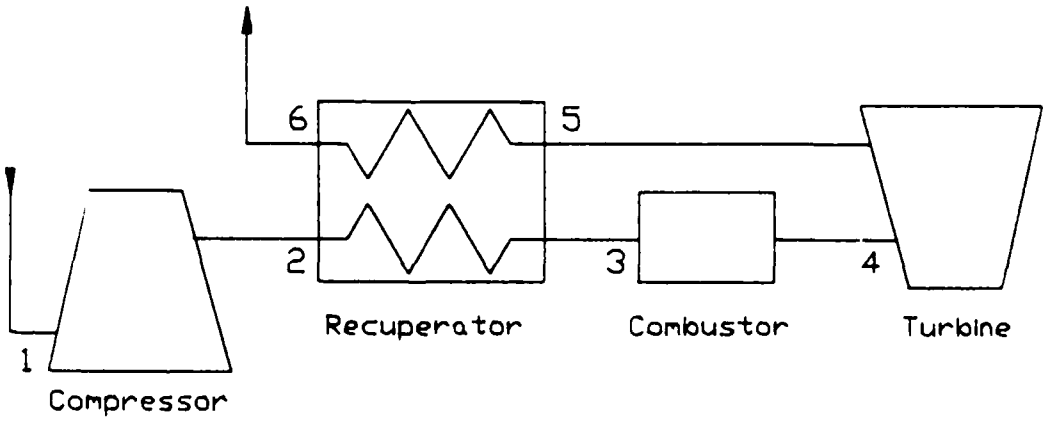

Regenerative Cycle Schematic
Figure 2.1

A compressor polytropic efficiency was assumed and used throughout all calculations, $\eta_{cp} = 0.95$. Similarly, a turbine polytropic efficiency was assumed, $\eta_{ct} = 0.90$. For ease of calculations, only one fluid was used, i.e., air was modeled as a perfect gas with $c_p = 1.0\ kj/kg - ^\circ K$ and $R = 0.287\ kj/kg - ^\circ K$ both assumed constant. The combustor, then, was treated as a perfect heat transfer device, but was not an injection point for fuel.

2.2 Cycle Parameters

A reasonable compressor inlet temperature was selected, $T_1 = 300^\circ K$, along with an inlet pressure of $P_1 = 1.126 \times 10^5 N/m^2$. A nominal value of turbine inlet temperature was also selected, $T_4 = 1300^\circ K$. The selection of an appropriate pressure ratio required the following consideration.

The addition of a recuperator to a simple open Brayton cycle causes a shift in the pressure ratio for maximum cycle efficiency from that of the non-regenerative cycle. A heat exchanger effectiveness of $\epsilon = 0.8$ was selected and cycle efficiency without losses was calculated for pressure ratios varying from 4 to 10. A sample calculation is contained in Appendix A, results are plotted in Figure 2.2.

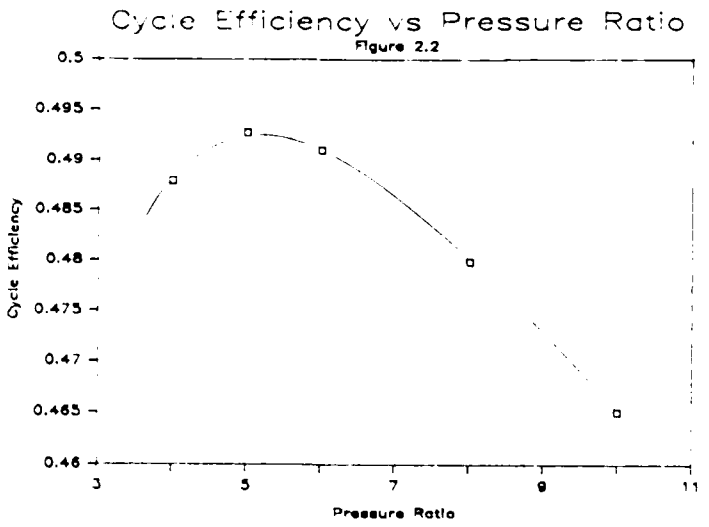

Based on these results, a pressure ratio of $P_2/P_1 = 5$ was selected. With this pressure ratio determined, the maximum cycle efficiency without losses, η_∞, could be calculated. This quantity will be used for comparison purposes and was computed as $\eta_\infty = 0.5760$.

2.3 Heat Exchanger Characteristics

A plate-fin heat exchanger surface was selected from those cataloged in reference [5]. Its characteristics and dimensions are shown in Figure 2.3. It has an uncomplicated geometry and a reasonably wide range of Reynolds numbers in which consistent results can be expected. The material is aluminum, with a thermal conductivity of $k_f = 190\ w/m - ^\circ K$.

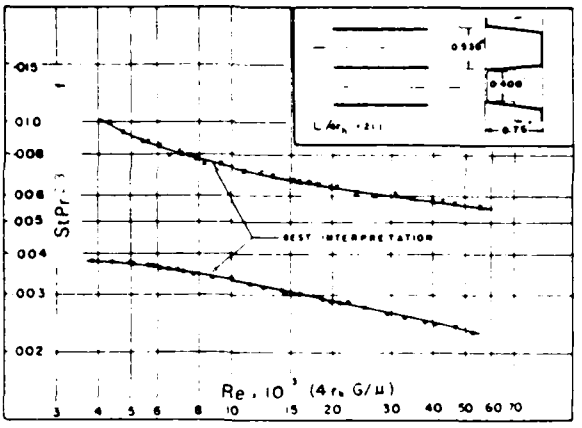

Fin pitch = 2.0 per in = 78.74 per m
Plate spacing, b = 0.750 in = 19.05 x 10^{-3} m
Fin length = 12.0 in = 304.8 x 10^{-3} m
Flow passage hydraulic diameter, $4r_h$ = 0.0474 ft = 14.453 x 10^{-3} m
Fin metal thickness = 0.032 in, aluminum = 0.813 x 10^{-3} m
Total heat transfer area/volume between plates, β = 76.1 ft^2/ft^3 = 249.672 m^2/m^3
Fin area/total area = 0.606

Plain Plate-Fin Surface 2.0
Figure 2.3

Chapter 3

CONVENTIONAL DESIGN METHOD

3.1 Introduction

This chapter outlines the conventional design procedure that was used to size the single-pass, counterflow gas-to-gas heat exchanger. This procedure was performed for various combinations of heat exchanger effectiveness and specified pressure drops. A complete numerical example is provided in Appendix B. Final results for this conventional method are shown in Table 3.1.

3.2 Conventional Methodology

For a single-pass counterflow design, when the core dimensions on one side are fixed, the dimensions on the other side are also known. This means the design is driven by the side that has the more stringent $\Delta P/P$ requirement. The method of determining the controlling side is contained in Appendix B. In every case considered, the hot side of the heat exchanger was the controlling side and so its requirements drove the design.

The following is a step-by-step heat exchanger sizing design procedure which closely follows that outlined in reference [2].

1. For the given heat exchanger effectiveness, determine the fluid outlet

temperatures. Calculate the fluid mean temperature on each side and evaluate fluid physical properties ρ_i, ρ_o, $(1/\rho)_m$, and μ.

2. Determine N_{tu} for the exchanger and then N_{tu} for each side. The influence of longitudinal heat conduction is ignored in this first iteration of design.

3. Estimate hot and cold side pressure drops, select an appropriate N_{Re}, and then a value of j/f from Figure 2.3.

4. Calculate mass velocity, G, from information in steps 1-3 and the corresponding value of $\Delta P/P$.

5. Calculate N_{Re} and determine values of j and f from Figure 2.3.

6. Compute heat transfer coefficient, h; temperature effectiveness of the fins, η_f; and the total surface temperature effectiveness, η_o.

7. Calculate heat transfer area, A; minimum free flow area, A_o; heat exchanger frontal area, A_{fr}; flow length, L; and heat exchanger volume, Vol.

8. Compute $\Delta P/P$ from known conditions and calculated parameters.

3.3 Analysis

For each case show in Table 3.1, cycle efficiency with losses, η, was calculated and the cycle efficiency degrade, $\eta_\infty - \eta$, is listed for each case. A correlation between heat exchanger effectiveness, ϵ, total allowed pressure drop, k, cycle efficiency degrade, and heat exchanger volume was sought.

The relationship between cycle efficiency degrade and effectiveness at various levels of k is shown in Figure 3.1. The increased level of degrade at lower values of effectiveness is as expected, and for a particular value of effectiveness, the degrade increases with increasing pressure drops.

The effects of varying effectiveness and pressure drops on heat exchanger volume is depicted in Figure 3.2. The higher the effectiveness, the longer

and therefore, larger the heat exchanger. Similarly, the greater pressure drop for a particular effectiveness also increases the volume.

Figure 3.3 was derived by extracting values of effectiveness at nominal values of $\eta_\infty - \eta$ and plotting them on the appropriate k curve of Figure 3.2. This resulted in curves of constant $\eta_\infty - \eta$ that have a minimum volume at a particular value of k and ϵ. It is emphasized that these "minimum" volumes were obtained at constant values of cycle degrade with varying pressure drops and effectiveness. These "minimum" volumes are plotted against effectiveness in Figure 3.4 with the respective k values annotated on the graph.

Case #	ϵ	k	$\eta_\infty - \eta$	L(m)	Vol (m^3)
C-1	1-0	0.02	0.0043	—	—
C-2	1.0	0.04	0.0089	—	—
C-3	1.0	0.06	0.0137	—	—
C-4	1.0	0.08	0.0188	—	—
C-5	0.9	0.0	0.0449	—	—
C-6	0.9	0.0240	0.0498	13.69	3.69
C-7	0.9	0.0388	0.0550	13.82	2.64
C-8	0.9	0.0558	0.0603	14.04	2.19
C-9	0.9	0.0739	0.0660	14.65	1.98
C-10	0.8	0.0	0.0833	—	—
C-11	0.8	0.0192	0.0886	6.15	1.12
C-12	0.8	0.0367	0.0941	6.56	0.85
C-13	0.8	0.0550	0.0999	6.72	0.71
C-14	0.8	0.0740	0.1060	7.15	0.65
C-15	0.7	0.0	0.1165	—	—
C-16	0.7	0.0188	0.1221	3.75	0.53
C-17	0.7	0.0365	0.1278	3.95	0.39
C-18	0.7	0.0565	0.1338	4.17	0.34
C-19	0.7	0.0734	0.1401	4.32	0.31
C-20	0.6	0.0	0.1455	—	—
C-21	0.6	0.0186	0.1512	2.52	0.29
C-22	0.6	0.0376	0.1571	2.69	0.22
C-23	0.6	0.0557	0.1632	2.85	0.19
C-24	0.6	0.0764	0.1695	2.98	0.17

Table 3.1: Conventional Method Results

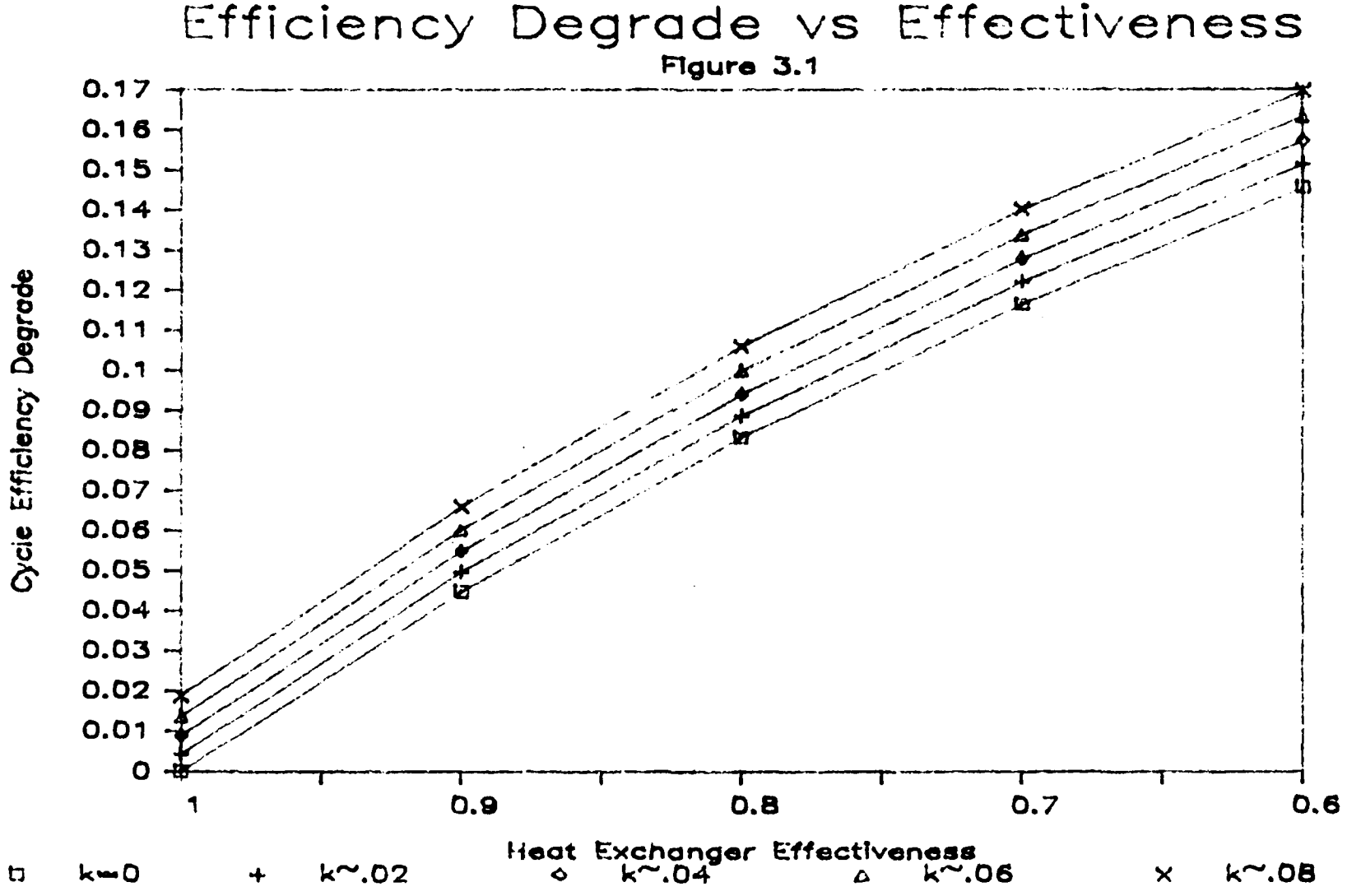
Efficiency Degrade vs Effectiveness
Figure 3.1
Cycle Efficiency Degrade
0.17
0.16
0.15
0.14
0.13
0.12
0.11
0.1
0.09
0.08
0.07
0.06
0.05
0.04
0.03
0.02
0.01
0
1
0.9
0.8
0.7
0.6
Heat Exchanger Effectiveness
k=0
k~.02
k~.04
k~.06
k~.08

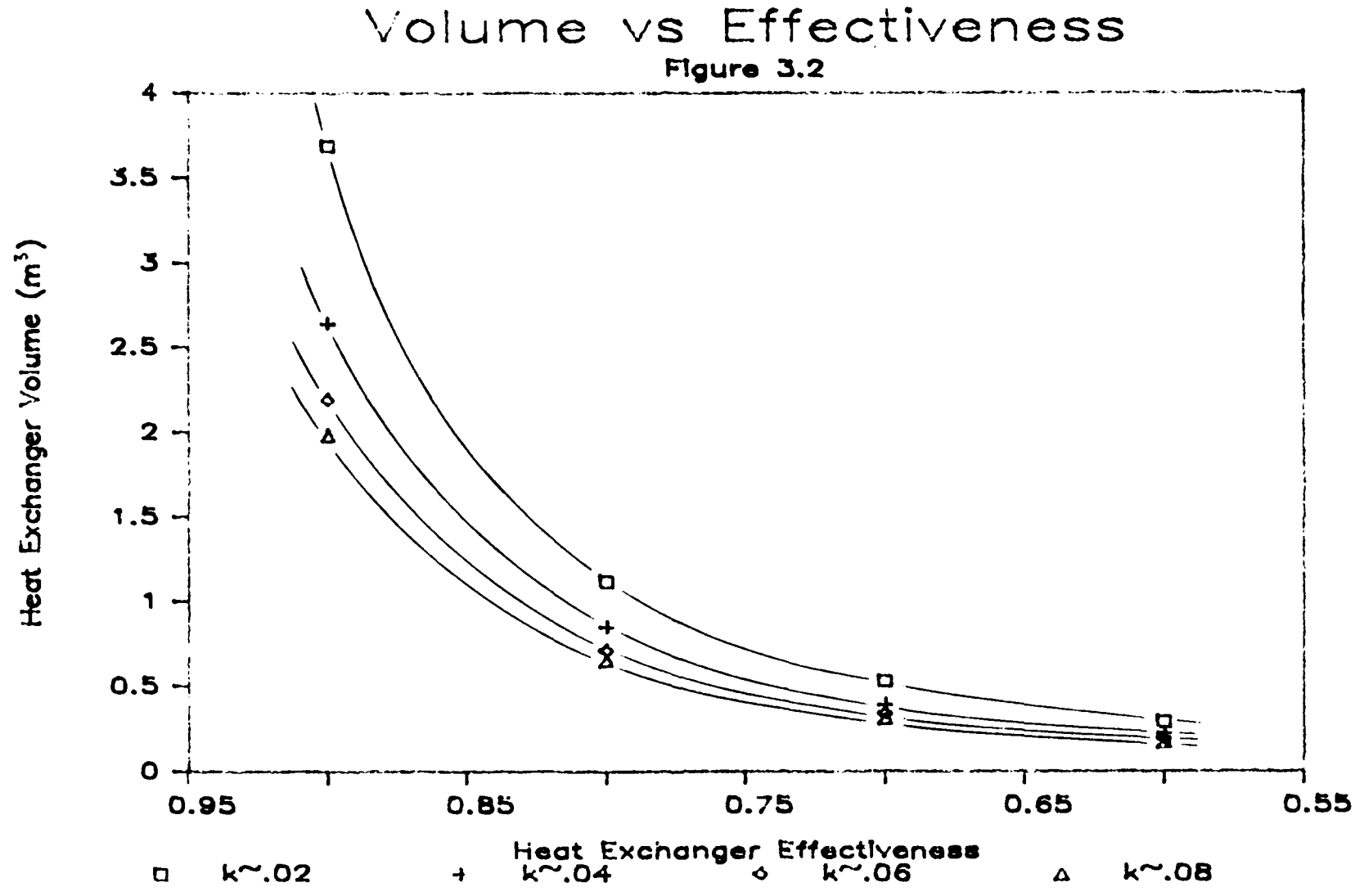
Volume vs Effectiveness
Figure 3.2
Heat Exchanger Volume (m^3)
4
3.5
3
2.5
2
1.5
1
0.5
0
0.95
0.85
0.75
0.65
0.55
Heat Exchanger Effectiveness
k~.02
k~.04
k~.06
k~.08

Volumes at Constant Cycle Degrade

Figure 3.3

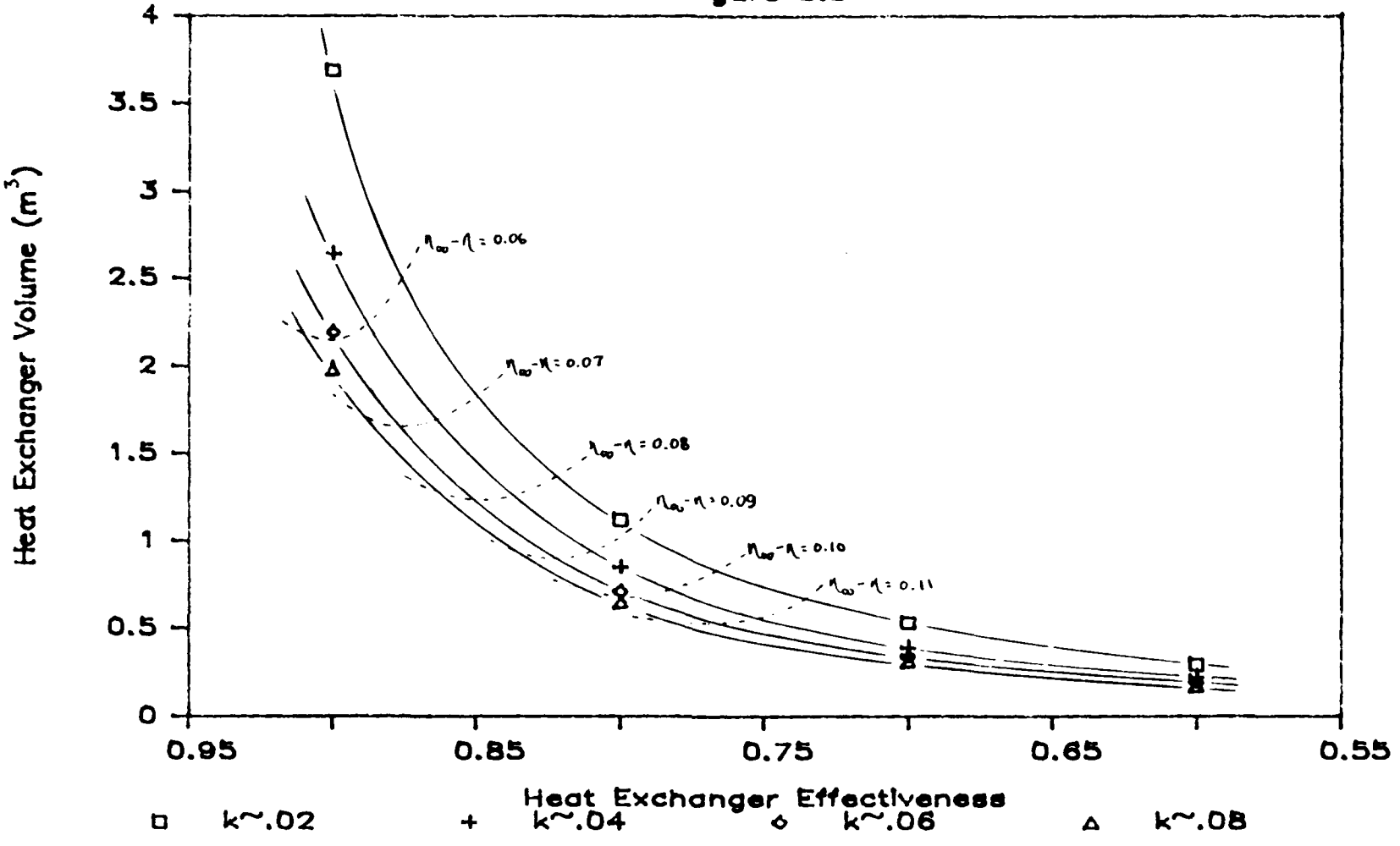

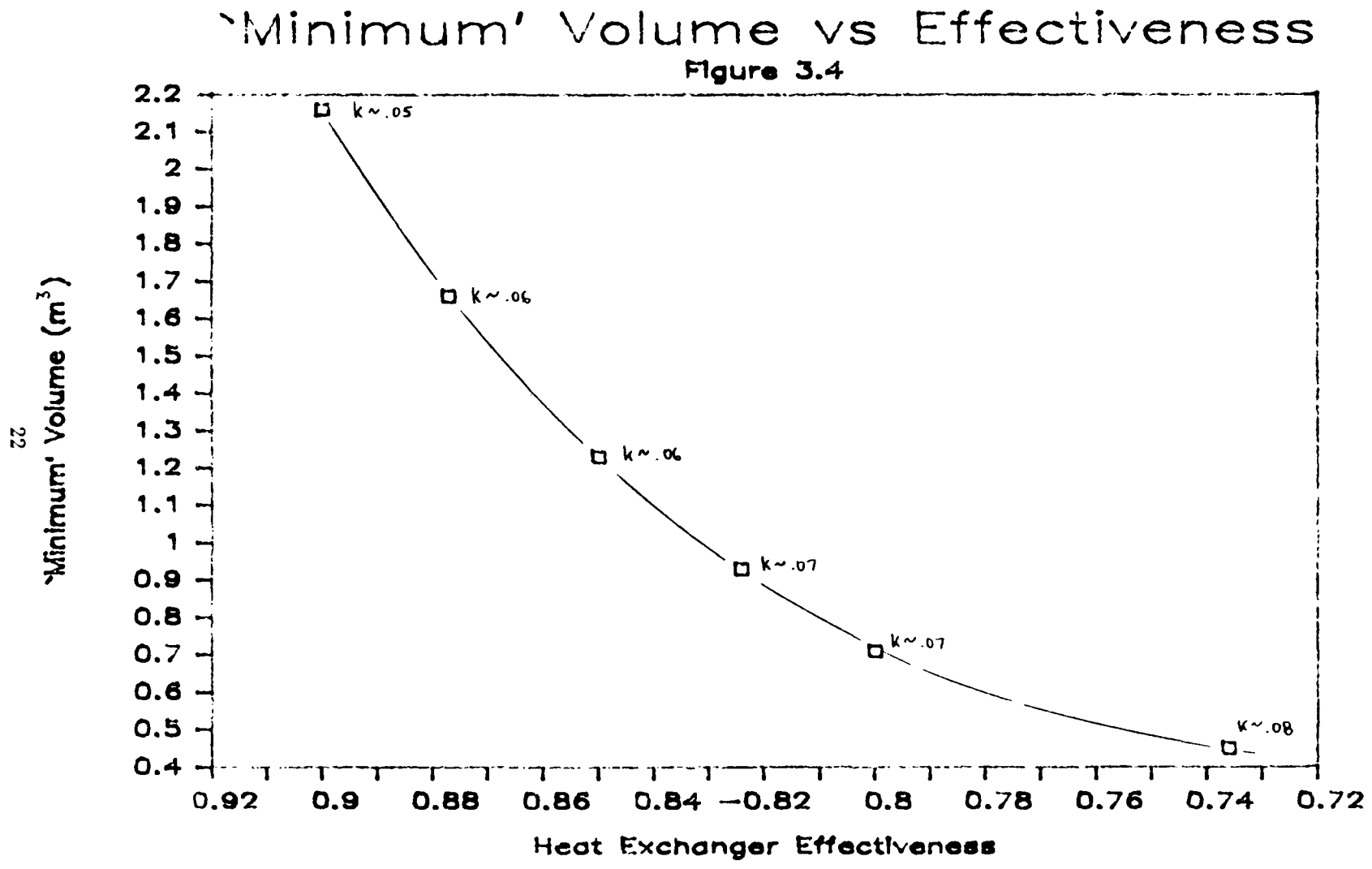
'Minimum' Volume vs Effectiveness
Figure 3.4
'Minimum' Volume (m^3)
2.2
2.1
2
1.9
1.8
1.7
1.6
1.5
1.4
1.3
1.2
1.1
1
0.9
0.8
0.7
0.6
0.5
0.4
k~.05
k~.06
k~.06
k~.07
k~.07
k~.08
0.92
0.9
0.88
0.86
0.84
0.82
0.8
0.78
0.76
0.74
0.72
Heat Exchanger Effectiveness

Chapter 4

MINIMUM ENTROPY DESIGN METHOD

4.1 Introduction

The use of irreversibility concepts in the design of the gas-to-gas counterflow heat exchanger will be presented in this chapter. For the same mass velocities that were used in Chapter 3, the heat exchanger geometric parameters can be determined to arrive at minimum levels of entropy generation. The outputs of this design procedure are heat exchanger effectiveness and the pressure loss suffered on each side. For a more detailed explanation of this procedure, the reader is directed to references [4] and [6].

4.2 Background

Since the method deals with the entropy generation within the recuperator, it is appropriate to begin with an entropy flux analysis on the control volume of the recuperator in Figure 4.1. The heat transfer from the outer walls is assumed to be negligible. The entropy generation rate can then be written as

$$\dot{S} = \dot{m}_1(s_{out} - s_{in})_1 + \dot{m}_2(s_{out} - s_{in})_2 \qquad (4.1)$$

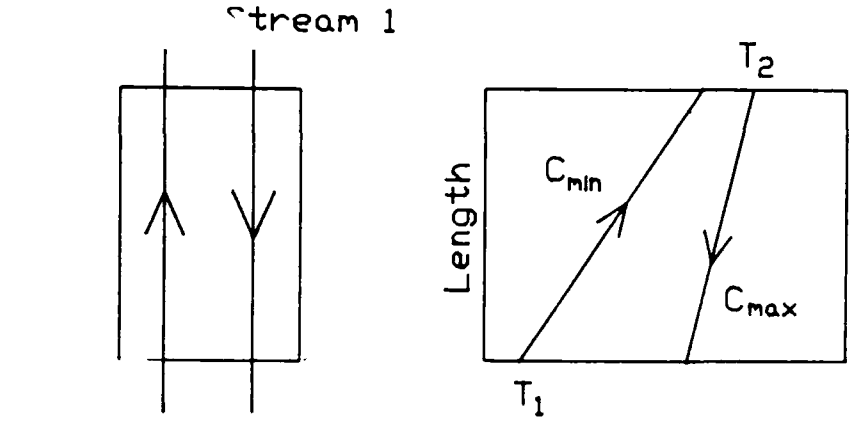

Recuperator Control Volume

Figure 4.1

Substituting expressions for the ideal gas entropy changes based on pressure and temperature relationships, this becomes

$$\dot{S} = C_{min}[ln(T_{1out}/T_1) + (R/C_p)_1 ln(P_1/P_{1out})]$$

$$+C_{max}[ln(T_{2out}/T_2) + (R/C_p)_2 ln(P_2/P_{2out})] \quad (4.2)$$

The number of entropy production units, N_s, is defined as

$$N_s = \dot{S}/C_{max} \quad (4.3)$$

Writing expressions for the first law of thermodynamics of the control volume,

$$C_{min}(T_1 - T_{1out}) + C_{min}(T_2 - T_{2out}) = 0 \quad (4.4)$$

and heat exchanger effectiveness,

$$\epsilon = (T_{1out} - T_1)/(T_2 - T_1) \quad (4.5)$$

permits the elimination of T_{1out} and T_{2out} in equation (4.2) which allows the rate of entropy production formula to be nondimensionalized as

$$N_s = \frac{C_{min}}{C_{max}} ln\left[1+\epsilon\left(\frac{T_2}{T_1}-1\right)\right] + ln\left[1-\frac{C_{min}}{C_{max}}\epsilon\left(1-\frac{T_1}{T_2}\right)\right]$$

$$-\frac{C_{min}}{C_{max}}\left(\frac{R}{C_p}\right)_1 ln\left(1-\frac{\Delta P}{P}\right)_1 - \left(\frac{R}{C_p}\right)_2 ln\left(1-\frac{\Delta P}{P}\right)_2 \qquad (4.6)$$

A special form of this last expression can be obtained in the case of nearly ideal heat exchangers. When the stream-to-stream ΔT's and frictional ΔP's are held small, two inequalities can be applied.

$$1-\epsilon \;<< 1 \qquad (4.7)$$

$$(\Delta P/P)_{1,2} \;<< 1 \qquad (4.8)$$

Applying these and expressing ϵ in terms of N_{tu} yields

$$N_s \simeq \frac{C_{min}}{C_{max}} ln\frac{T_2}{T_1} + ln\left[1-\frac{C_{min}}{C_{max}}\left(1-\frac{T_1}{T_2}\right)\right]$$

$$+ \left(\frac{C_{min}}{C_{max}}\right)^2\left(1-\frac{C_{min}}{C_{max}}\right)\frac{\left(1-\frac{T_1}{T_2}\right)^2}{1-\frac{C_{min}}{C_{max}}\left(1-\frac{T_1}{T_2}\right)}\frac{exp\left[-N_{tu}\left(1-\frac{C_{min}}{C_{max}}\right)\right]}{1-\frac{C_{min}}{C_{max}}exp\left[-N_{tu}\left(1-\frac{C_{min}}{C_{max}}\right)\right]}$$

$$+ \frac{C_{min}}{C_{max}}\left(\frac{R}{C_p}\right)_1\left(\frac{\Delta P}{P}\right)_1 + \left(\frac{R}{C_p}\right)_2\left(\frac{\Delta P}{P}\right)_2 \qquad (4.9)$$

The first two terms can be characterized as a contribution from capacity rate imbalance, the third represents contribution due to finite N_{tu}, and the last two show fluid friction effects.

Requiring the streams to be balanced and applying the calculus of limits as $C_{min} \rightarrow C_{max}$, equation (4.9) can be reduced to

$$N_s \simeq \frac{C_{min}}{C_{max}} ln\frac{T_2}{T_1} + ln\left[1-\frac{C_{min}}{C_{max}}\left(1-\frac{T_1}{T_2}\right)\right] + \left(\sqrt{\frac{T_2}{T_1}}-\sqrt{\frac{T_1}{T_2}}\right)^2\frac{1}{N_{tu}}$$

$$+ \quad \frac{C_{min}}{C_{max}} \left(\frac{R}{C_p}\right)_1 \left(\frac{\Delta P}{P}\right)_1 + \left(\frac{R}{C_p}\right)_2 \left(\frac{\Delta P}{P}\right)_2 \qquad (4.10)$$

When the overall N_{tu} is expressed in terms of N_{tu} for each side of the heat transfer surface,

$$\frac{1}{N_{tu}} = \frac{1}{N_{tu1}} + \frac{C_{min}}{C_{max}} \frac{1}{N_{tu2}} \qquad (4.11)$$

the number of entropy generation units can be divided into three contributions

$$N_s \simeq N_{s\,imbalance} + N_{s1} + N_{s2} \qquad (4.12)$$

Applying the limit $C_{min} \rightarrow C_{max}$, the imbalance terms of equation (4.10) can be written as

$$N_{s\,imbalance} = \left(\frac{C_{max}}{C_{min}} - 1\right) \left(\frac{T_2}{T_1} - 1 - \frac{C_{min}}{C_{max}} ln \frac{T_2}{T_1}\right) \qquad (4.13)$$

which will clearly vanish when $C_{min} = C_{max}$. Since this is the case for the design here, the number of entropy production units for each side can be determined from

$$N_{s1} = \left(\sqrt{\frac{T_2}{T_1}} - \sqrt{\frac{T_1}{T_2}}\right)^2 \frac{1}{N_{tu1}} + \left(\frac{R}{C_p}\right)_1 \left(\frac{\Delta P}{P}\right)_1 \qquad (4.14)$$

$$N_{s2} = \left(\sqrt{\frac{T_2}{T_1}} - \sqrt{\frac{T_1}{T_2}}\right)^2 \frac{1}{N_{tu2}} + \left(\frac{R}{C_p}\right)_2 \left(\frac{\Delta P}{P}\right)_2 \qquad (4.15)$$

4.3 Design Considerations

The number of entropy generation units that have been deemed acceptable for a particular design is a function of the hydraulic radius, minimum free flow area and flow length. It is necessary, then, to express N_s in terms of these and other known flow parameters. Using the definitions of N_{tu} and friction factor for each side

$$N_{tu1,2} = (L/r_h) N_{st} \qquad (4.16)$$

$$(\Delta P/P)_{1,2} = f(L/r_h) G^2/(2\rho P) \qquad (4.17)$$

in equations (4.14) and (4.15) leads to

$$N_{s1,2} = \frac{a\tau}{(L/r_h)N_{st}} + bBf(L/r_h)g^2 \tag{4.18}$$

where

$$\begin{aligned} a_1 &= 1 \\ a_2 &= C_{min}/C_{max} \end{aligned} \tag{4.19}$$

$$\begin{aligned} b_1 &= C_{min}/C_{max} \\ b_2 &= 1 \end{aligned} \tag{4.20}$$

$$B_1 = (R/C_p)_1$$

$$B_2 = (R/C_p)_2 \tag{4.21}$$

$$\tau = \left(\sqrt{\frac{T_2}{T_1}} - \sqrt{\frac{T_1}{T_2}}\right)^2 \tag{4.22}$$

$$g = G/(2\rho P)^{\frac{1}{2}} \tag{4.23}$$

As can be seen in equation (4.18), the ratio L/r_h performs a trade-off function, i.e., for a fixed g and N_{Re}, there will be an optimum L/r_h which results in a minimum $N_{s1,2}$. When the function $N_{s1,2}$ is minimized, the $(L/r_h)_{opt}$ is given by

$$(L/r_h)_{opt} = \frac{2}{G}\left(\frac{\tau/N_{st}}{Bf(1/\rho_c P_c + 1/\rho_h P_h)}\right)^{\frac{1}{2}} \tag{4.24}$$

4.4 Minimum Entropy Design Methodology

The method used is based on optimizing (L/r_h). Since r_h is set by the selection of the plate-fin surface, this yields a length that will produce minimum entropy for the given hydraulic radius.

The following outlines the methodology employed. A complete numerical example is shown in Appendix C. Final results for all cases are tabulated in Table 4.1.

1. For the cases listed in Table 3.1 that resulted in a heat exchanger volume, use calculated G and N_{Re} to determine $(L/r_h)_{opt}$.

2. Compute resultant heat exchanger effectiveness and hot and cold side pressure drops.

3. Calculate N_{s_h}, N_{s_c}, and $N_{s_{total}}$.

4. Calculate the heat exchanger volume for each case.

5. Determine the cycle efficiency degrade, $\eta_\infty - \eta$.

4.5 Analysis

Figure 4.2 shows the nearly linear relationship of cycle efficiency degrade and heat exchanger effectiveness. There is not the clear definition of different values of pressure drop as was observed for the conventional method in Figure 3.1. In fact, there is even a wider range of k values here, from $k = 0.056$ for case E-6 to $k = 0.269$ for case E-24, and yet the results are almost linear across that range.

The volume plotted in Figure 4.3 is that volume obtained by minimizing entropy generation in the heat exchanger and should not be interpreted as a minimum volume, but rather as an "optimum" volume for minimizing entropy generation.

To achieve a better basis for comparison of the two methods, the entropy generated by the various designs must be discussed.

Case #	$L_{opt}(m)$	Vol(m^3)	k	ϵ	$\eta_\infty - \eta$	N_s
E-6	32.03	8.63	0.0563	0.955	0.0347	0.0325
E-7	25.86	4.93	0.0727	0.945	0.0440	0.0417
E-8	22.04	3.44	0.0876	0.935	0.0528	0.0503
E-9	20.12	2.72	0.1014	0.926	0.0606	0.0583
E-11	24.35	4.46	0.07658	0.942	0.0461	0.0441
E-12	19.08	2.46	0.1069	0.922	0.0641	0.0614
E-13	16.11	1.07	0.1320	0.908	0.0784	0.0760
E-14	15.08	1.38	0.1559	0.896	0.0917	0.0897
E-16	19.80	2.77	0.996	0.927	0.0596	0.0573
E-17	15.40	1.53	0.1422	0.902	0.0844	0.0823
E-18	13.19	1.07	0.1778	0.884	0.105	0.1028
E-19	12.11	0.86	0.2058	0.872	0.1211	0.1189
E-21	16.98	1.93	0.1252	0.913	0.0741	0.0718
E-22	12.87	1.04	0.1799	0.882	0.1067	0.1048
E-23	11.52	0.76	0.2251	0.862	0.1335	0.1309
E-24	10.47	0.60	0.2685	0.847	0.1596	0.1541

Table 4.1: Entropy Generation Method Results

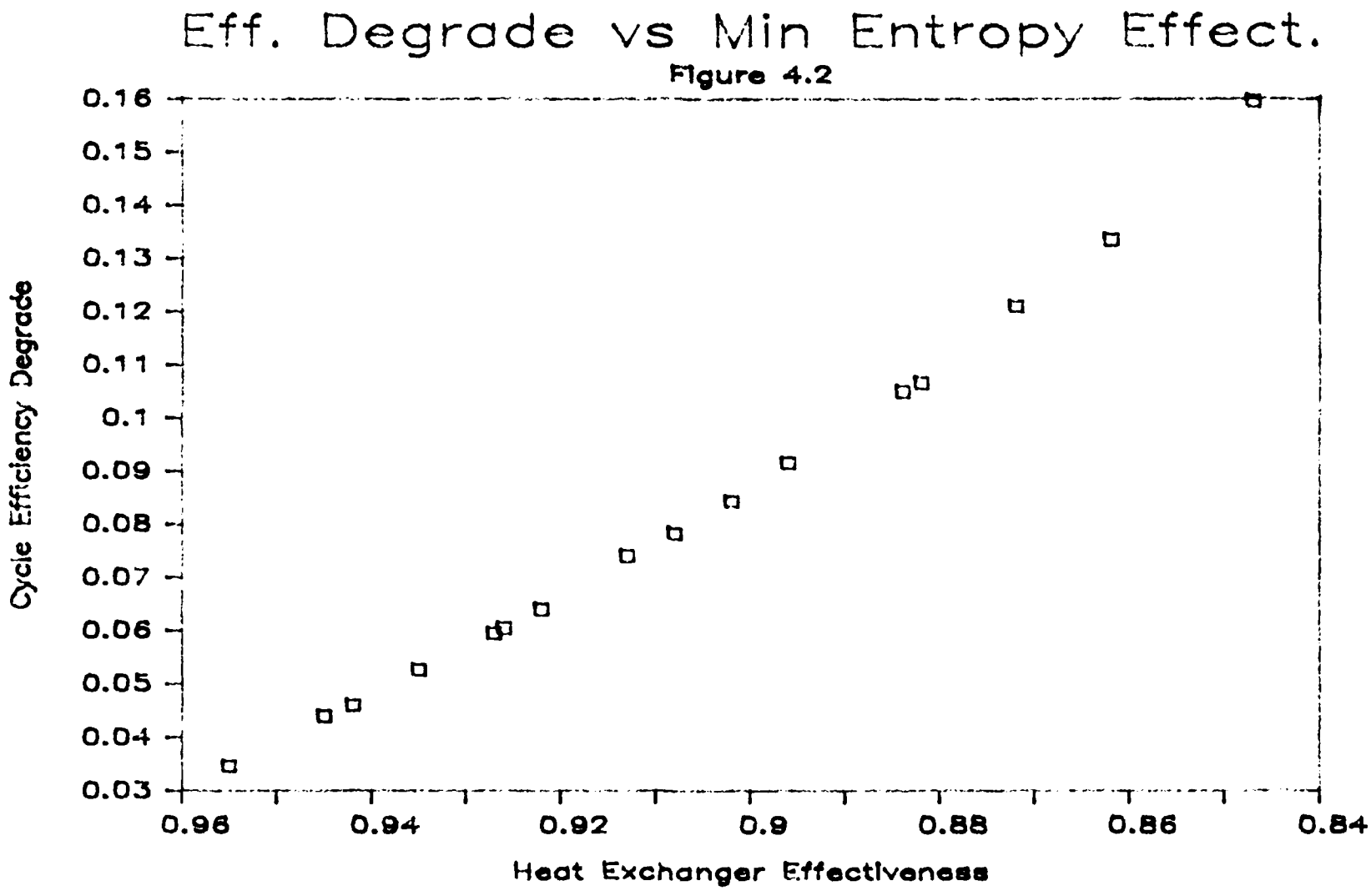
Eff. Degrade vs Min Entropy Effect.
Cycle Efficiency Degrade
0.16
0.15
0.14
0.13
0.12
0.11
0.1
0.09
0.08
0.07
0.06
0.05
0.04
0.03
0.96
0.94
0.92
0.9
0.88
0.86
0.84
Heat Exchanger Effectiveness

Figure 4.2

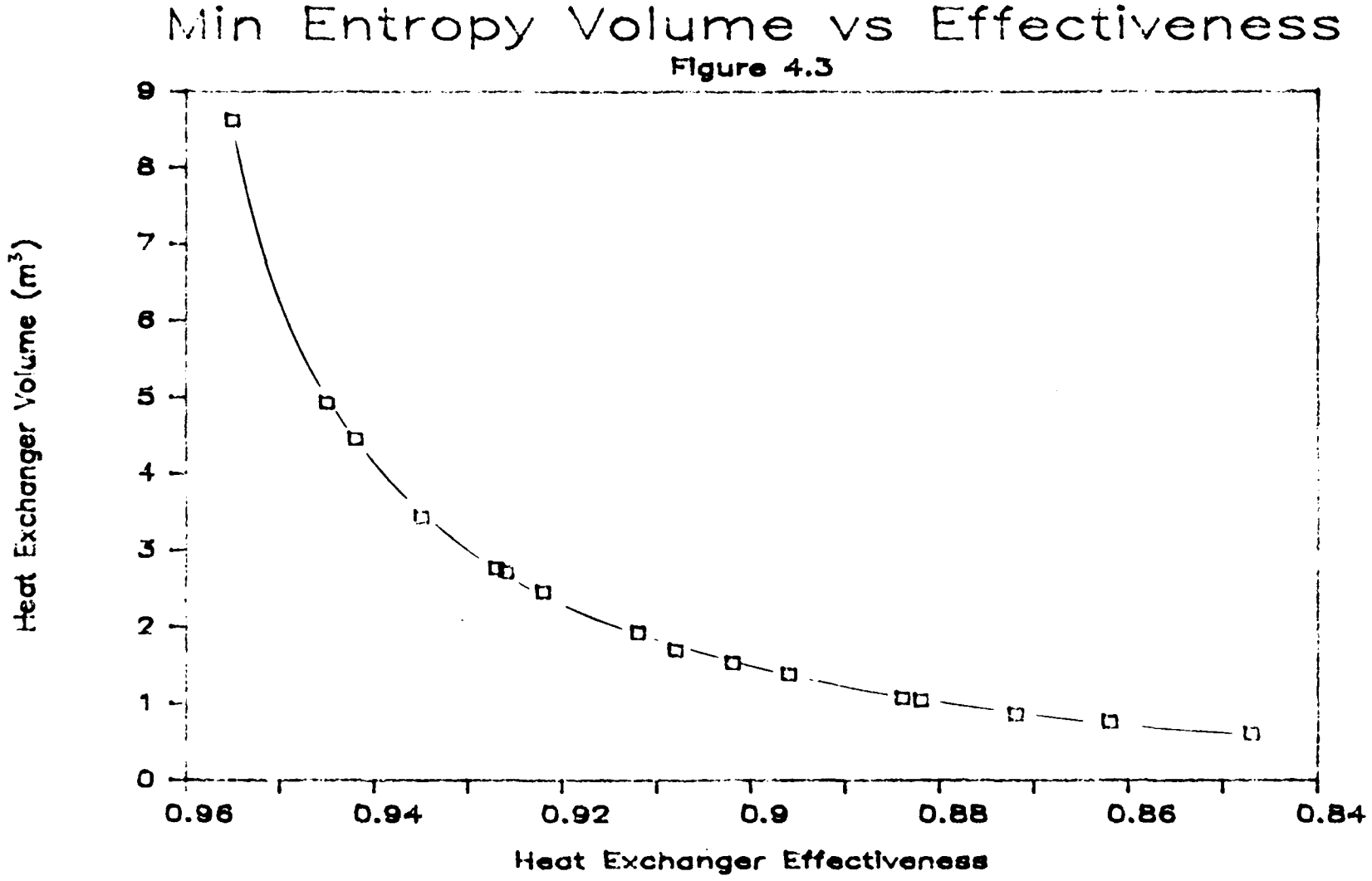
Min Entropy Volume vs Effectiveness
Figure 4.3
Heat Exchanger Volume (m³)
9
8
7
6
5
4
3
2
1
0
0.96
0.94
0.92
0.9
0.88
0.86
0.84
Heat Exchanger Effectiveness

Chapter 5

COMPARISONS AND RESULTS

5.1 Introduction

To this point, the minimum entropy method results have been compared to the conventional method results in terms of conventional method standards, i.e., pressure drops, efficiencies, and effectiveness. It is necessary to compare these methods in terms of the minimum entropy method, i.e., the entropy generated in each design.

5.2 Conventional Method Entropy Generation

The number of entropy generation units for each design can be computed from previously determined information and equations (4.14) and (4.15). An example of these calculations is contained in Appendix D. Results for the conventional cases are listed in Table 5.1. The large deviation in N_s and $\eta_\infty - \eta$ for cases C-21 through C-24 are a result of violating the assumption that $1 - \epsilon << 1$. These conventional cases will be discarded from further consideration. However, the minimum entropy cases at corresponding mass velocities are still valid.

When the entropy generation units are plotted against the degrade in cycle efficiency, Figure 5.1, the dependence on pressure drop is still present.

The grouping of data points is caused by the discrete changes in heat exchanger effectiveness, decreasing from left to right.

Figure 5.2 was created by using the same values of $\eta_\infty - \eta$ that were used for Figure 3.4. The value of N_s at each of these cycle efficiency degrades was read off at a particular value of k. Plotting these "minimum" volumes against entropy generation rate exhibits the general trend that the larger the volume of the heat exchanger, the lower the total entropy generated. This is in consonance with the results predicted by reference [4].

5.3 Minimum Entropy Generation

The cycle efficiency degrade vs. entropy generated for the minimum entropy method is similar in overall shape to that of the conventional method, but, as Figure 5.3 shows, the relationship is nearly linear and does not show the discrete pressure drop differences.

Figure 5.4 shows that the "optimum" volumes determined by$(L/r_h)_{opt}$ follow essentially the same path as that of the conventional method. For a direct comparison, Figures 5.2 and 5.4 are plotted together on Figure 5.5.

To ensure that the $(L/r_h)_{opt}$ expression, (4.24), was giving minimum entropy results, a series of calculations was performed at (L/r_h) values on both sides of the optimum for case E-9. Figure 5.6 shows that the minimum entropy solution was, in fact, being determined. It is also noted that the magnitudes of N_s and $\eta_\infty - \eta$ are essentially the same over this range of heat exchanger effectiveness.

5.4 Comparisons

The calculations performed on case E-9 to prove minimization also yielded heat exchanger volumes at a constant mass velocity G. These additional data points are plotted on Figure 5.7. The dash-dot line connecting them is a locus of recuperator volumes along a constant G path. This shows why the volumes at minimum N_s or $\eta_\infty - \eta$ along a constant G path are larger that the miminum volume of a given N_s or $\eta_\infty - \eta$.

Figure 5.8 shows a comparison between conventional "minimum" volumes and minimum entropy "optimum" volumes. The minimum entropy method yields volumes that are larger than the conventional method for the same cycle efficiency degrade.

Case #	$\eta_\infty - \eta$	N_s
C-1	0.0043	—
C-2	0.0089	—
C-3	0.0137	—
C-4	0.0188	—
C-5	0.0449	—
C-6	0.0498	0.0445
C-7	0.0550	0.0494
C-8	0.0603	0.0550
C-9	0.0660	0.0610
C-10	0.0833	—
C-11	0.0886	0.0900
C-12	0.0941	0.0967
C-13	0.0999	0.1036
C-14	0.1060	0.1108
C-15	0.1165	—
C-16	0.1221	0.1505
C-17	0.1278	0.1584
C-18	0.1338	0.1669
C-19	0.1401	0.1748
C-20	0.1455	—
C-21	0.1512	0.2308
C-22	0.1571	0.2405
C-23	0.1632	0.2501
C-24	0.1695	0.2607

Table 5.1: Conventional Method Entropy Generation

Efficiency Degrade vs Entropy Generated

Figure 5.1

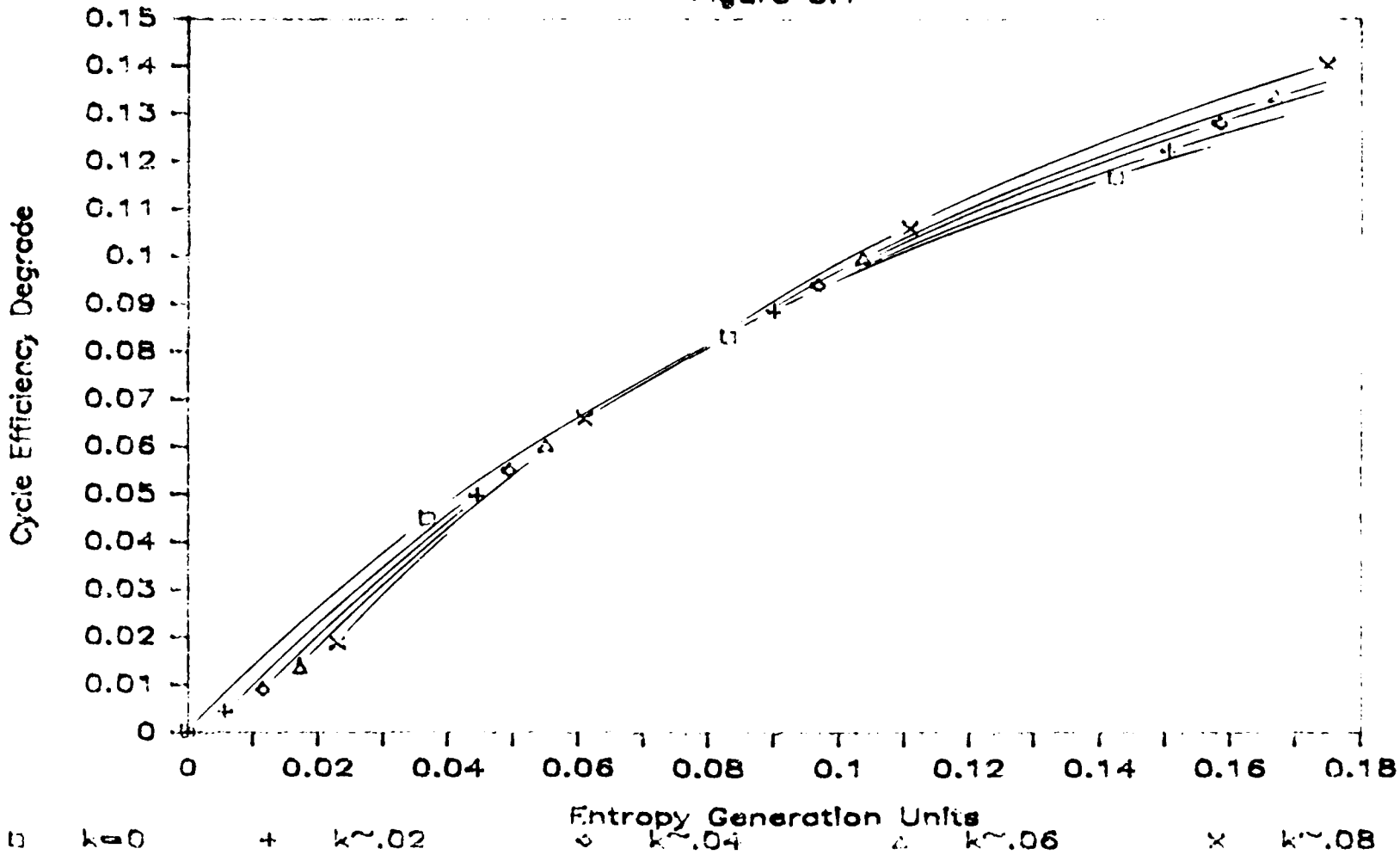

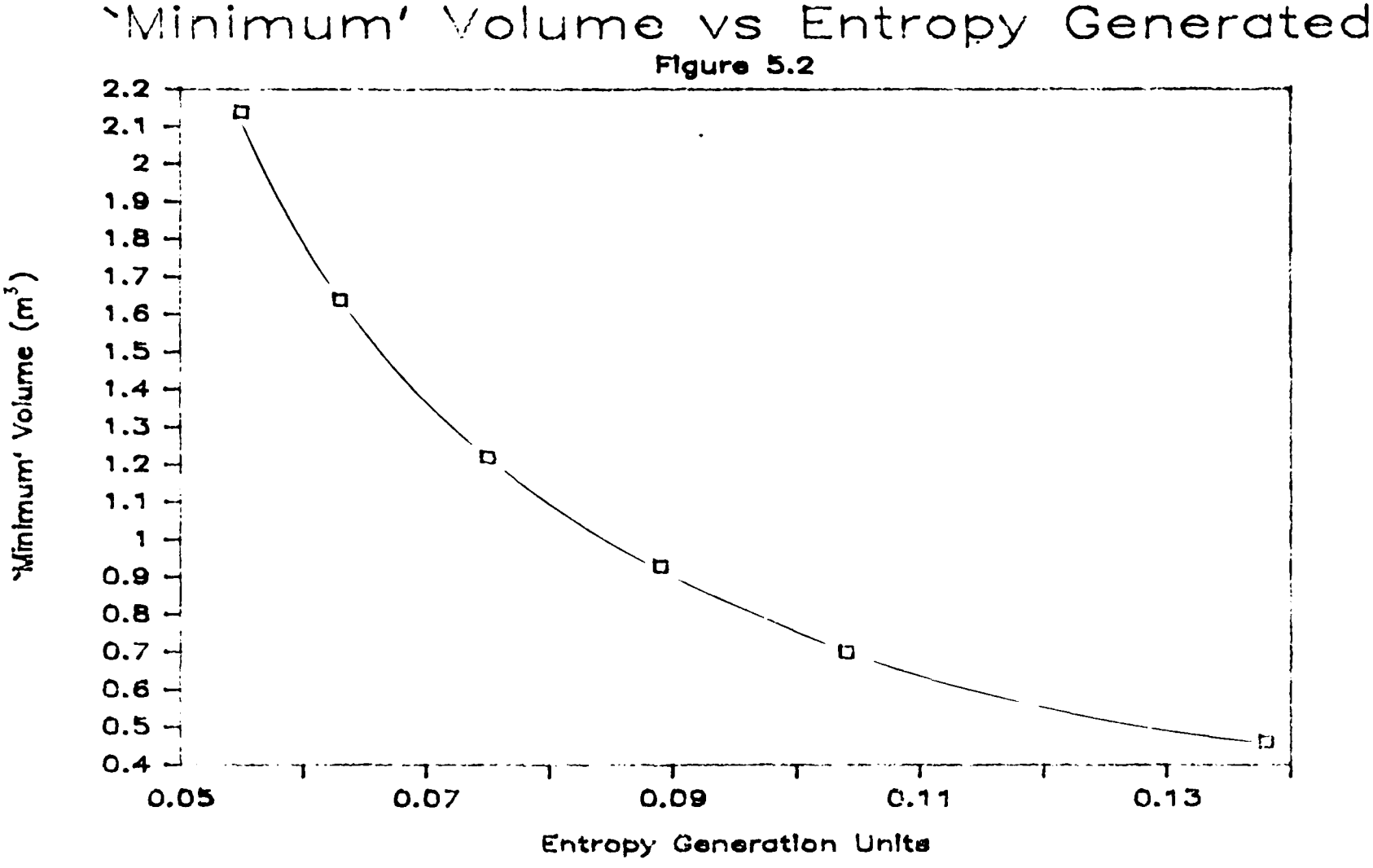
'Minimum' Volume vs Entropy Generated
'Minimum' Volume (m^3)
2.2
2.1
2
1.9
1.8
1.7
1.6
1.5
1.4
1.3
1.2
1.1
1
0.9
0.8
0.7
0.6
0.5
0.4
0.05
0.07
0.09
0.11
0.13
Entropy Generation Units

Figure 5.2

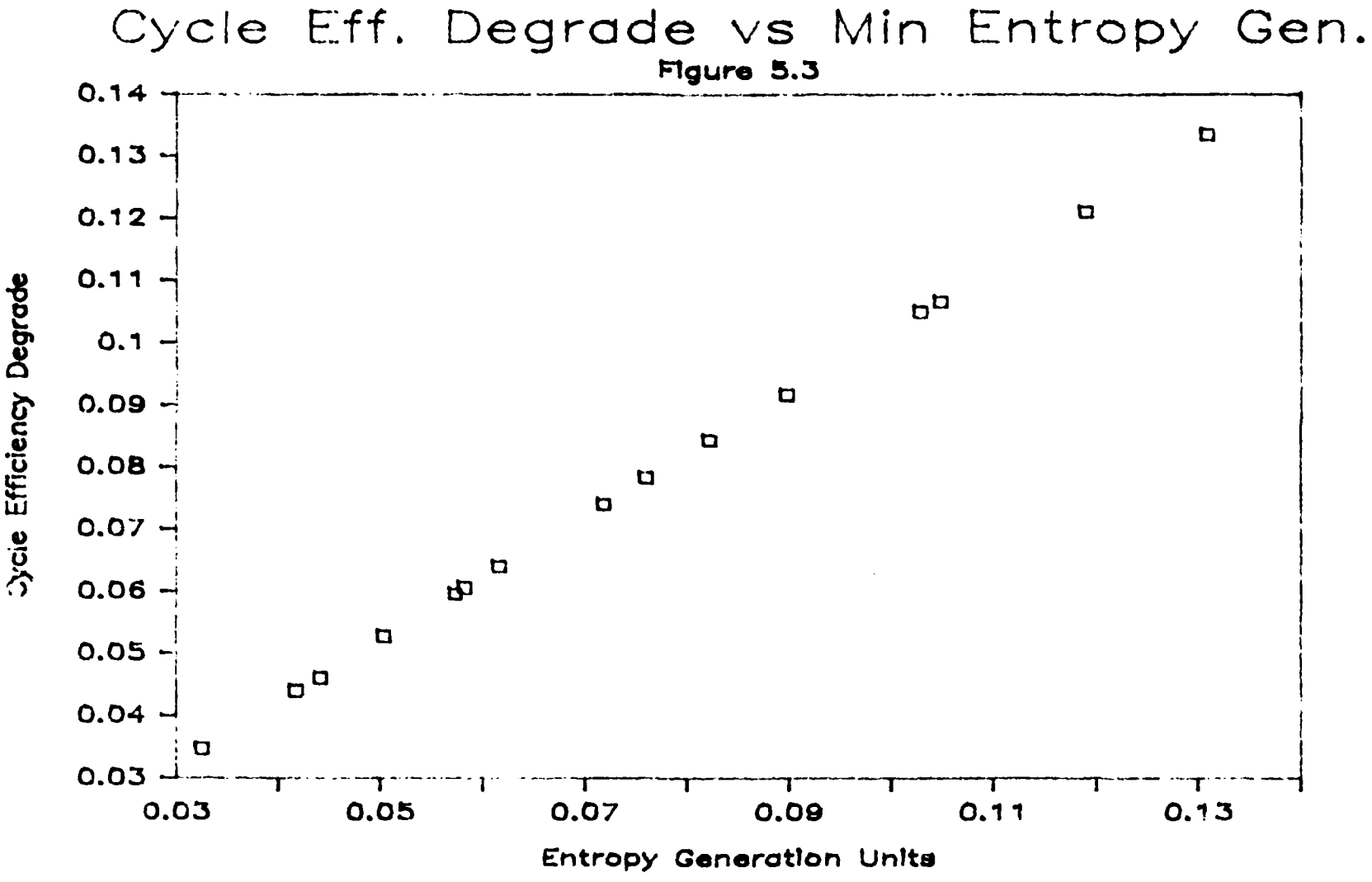
Cycle Eff. Degrade vs Min Entropy Gen.
Figure 5.3
Cycle Efficiency Degrade
0.14
0.13
0.12
0.11
0.1
0.09
0.08
0.07
0.06
0.05
0.04
0.03
0.03
0.05
0.07
0.09
0.11
0.13
Entropy Generation Units

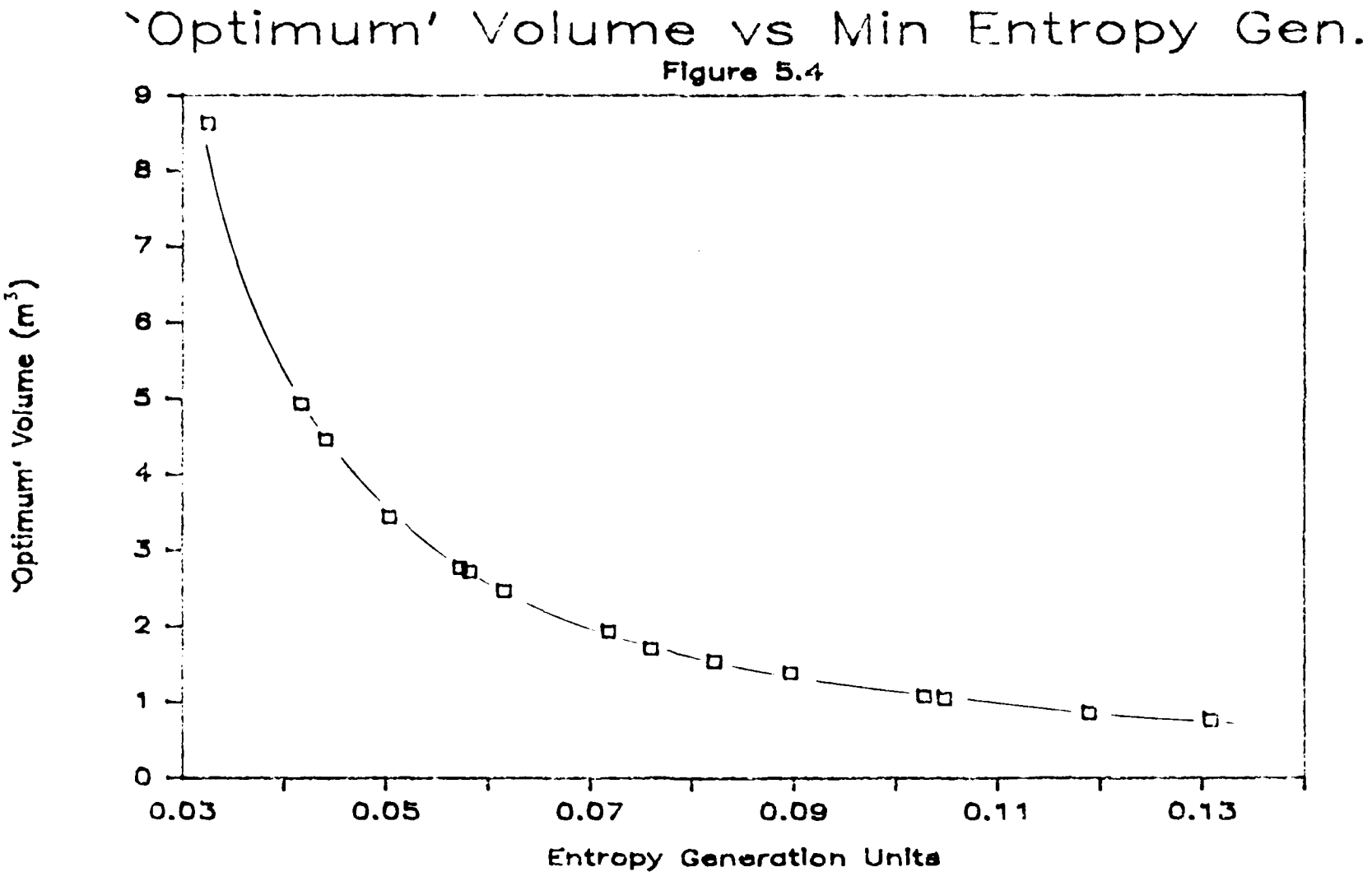
'Optimum' Volume vs Min Entropy Gen.
'Optimum' Volume (m^3)
9
8
7
6
5
4
3
2
1
0
0.03
0.05
0.07
0.09
0.11
0.13
Entropy Generation Units

Figure 5.4

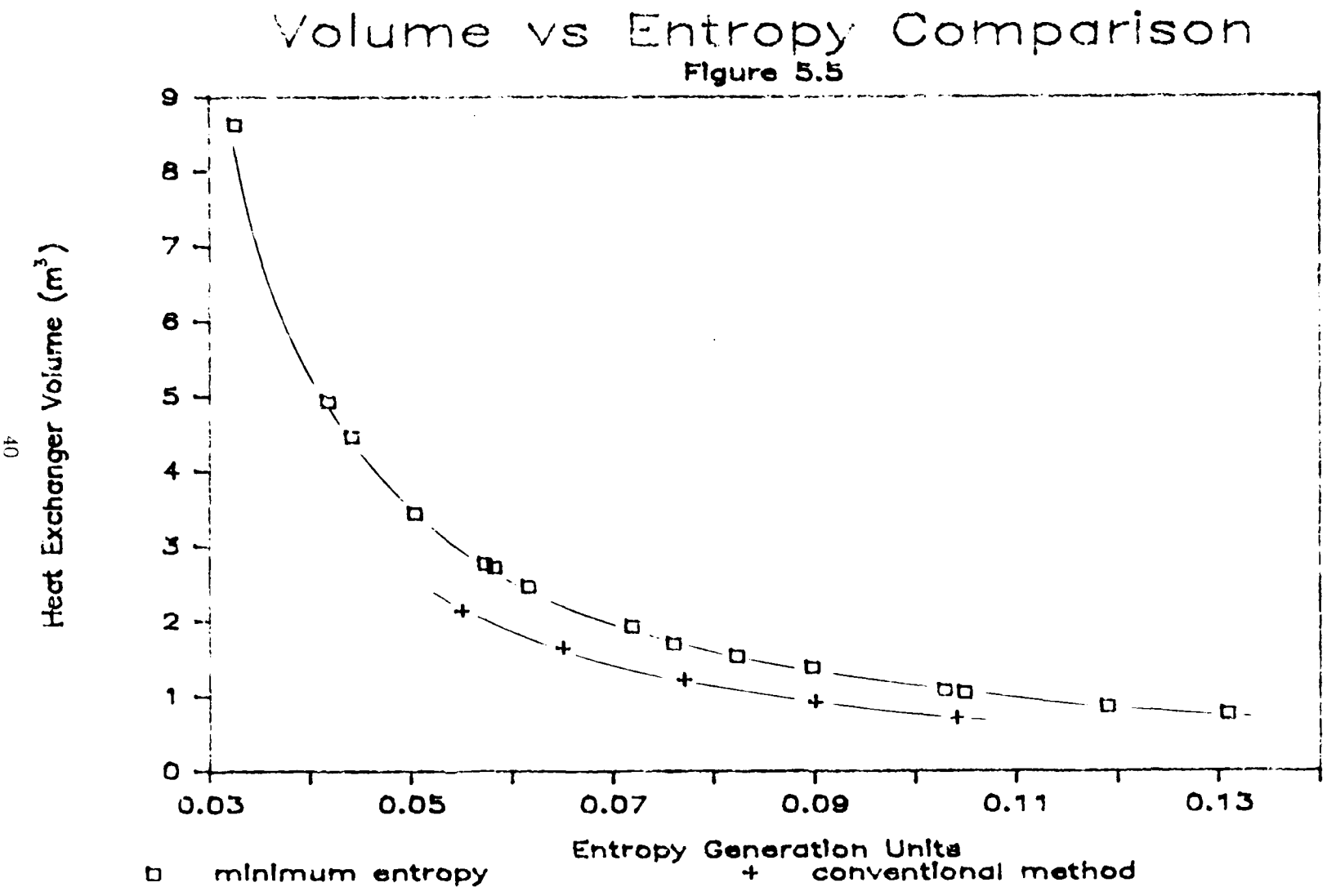
Volume vs Entropy Comparison
Heat Exchanger Volume (m^3)
9
8
7
6
5
4
3
2
1
0
0.03
0.05
0.07
0.09
0.11
0.13
Entropy Generation Units
minimum entropy
conventional method

Figure 5.5

Case E-9 (L/r_h) Optimization

Figure 5.6

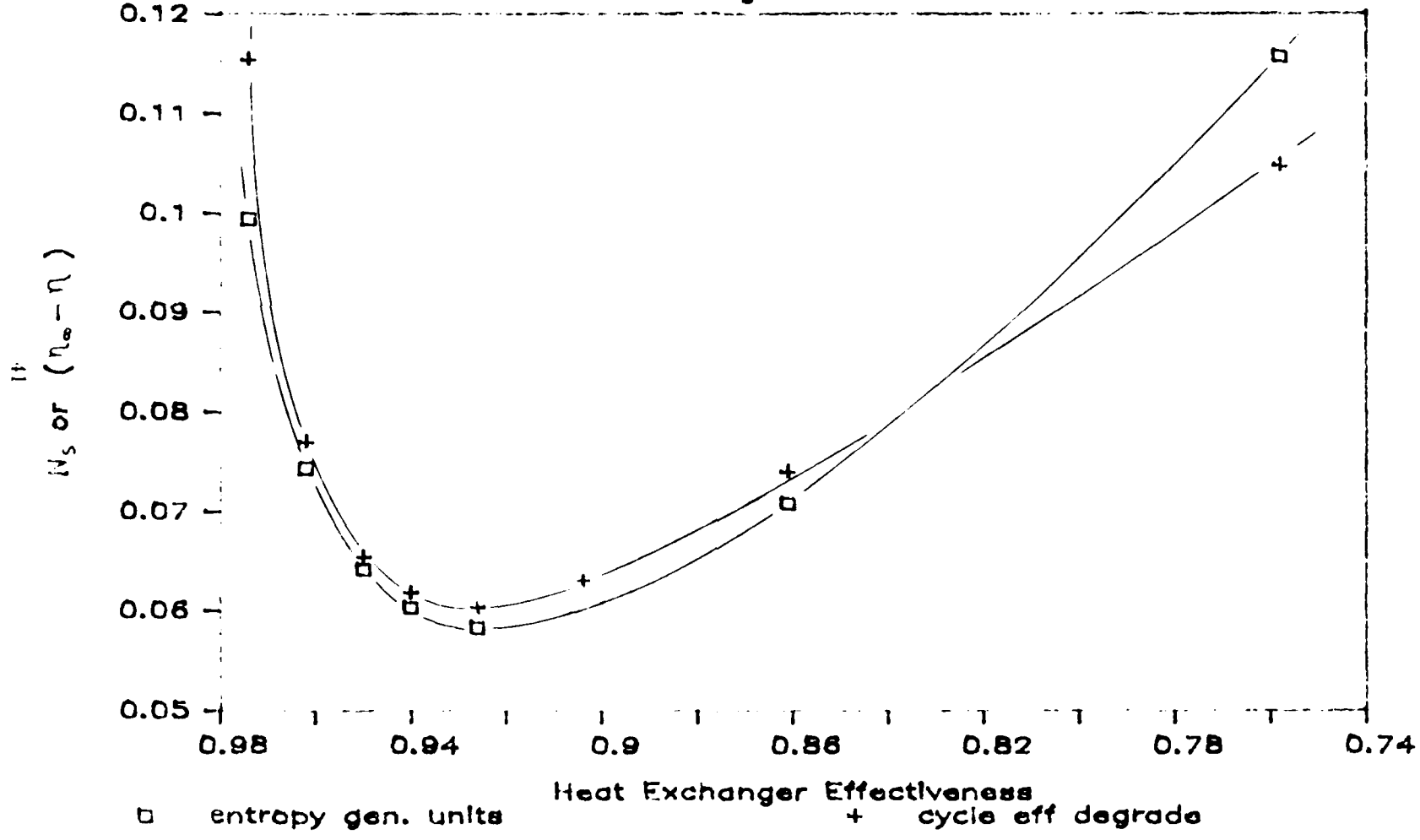

Volumes along Constant G Path

Figure 5.7

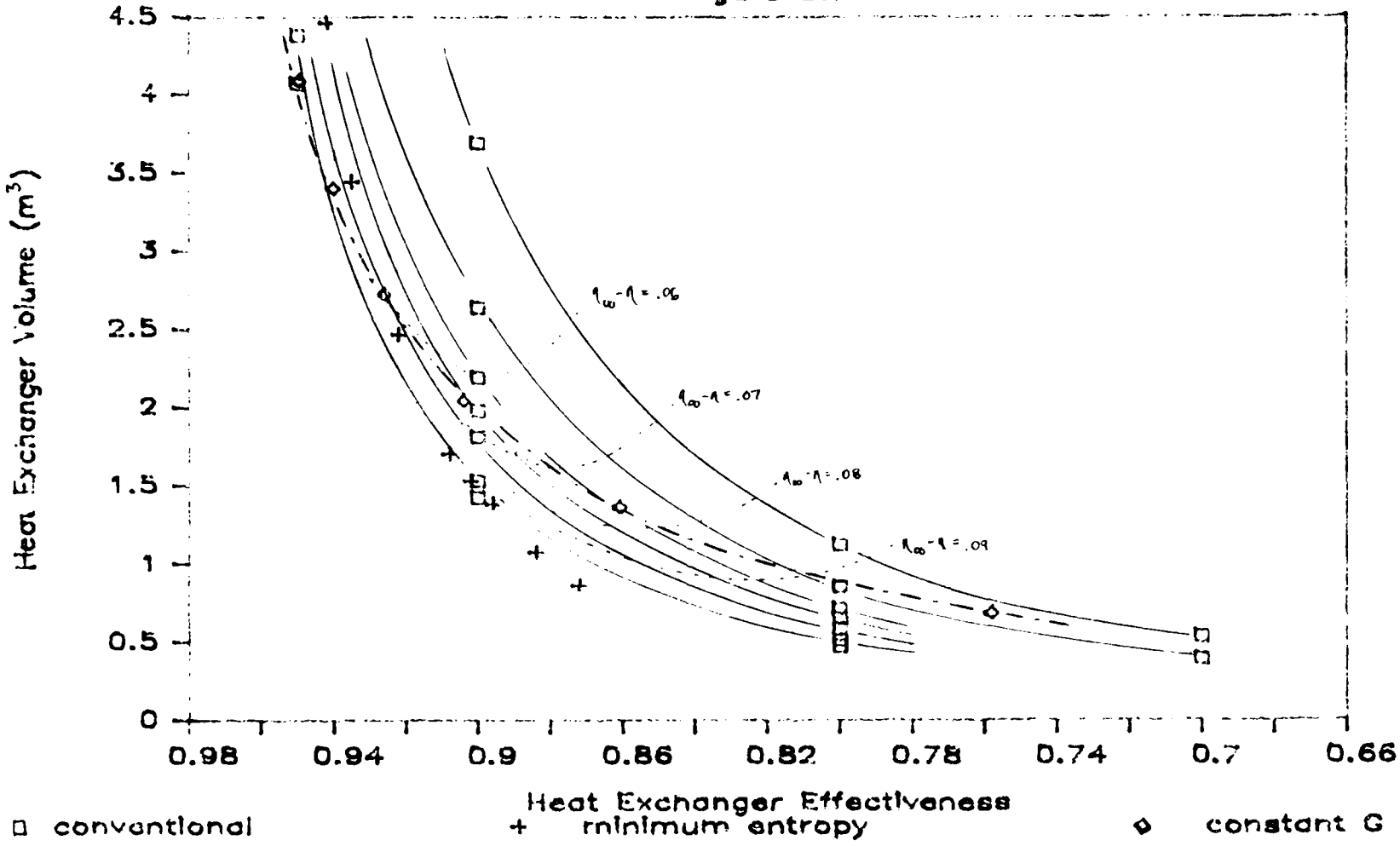

Volume vs Eff. Degrade Comparison

Figure 5.8

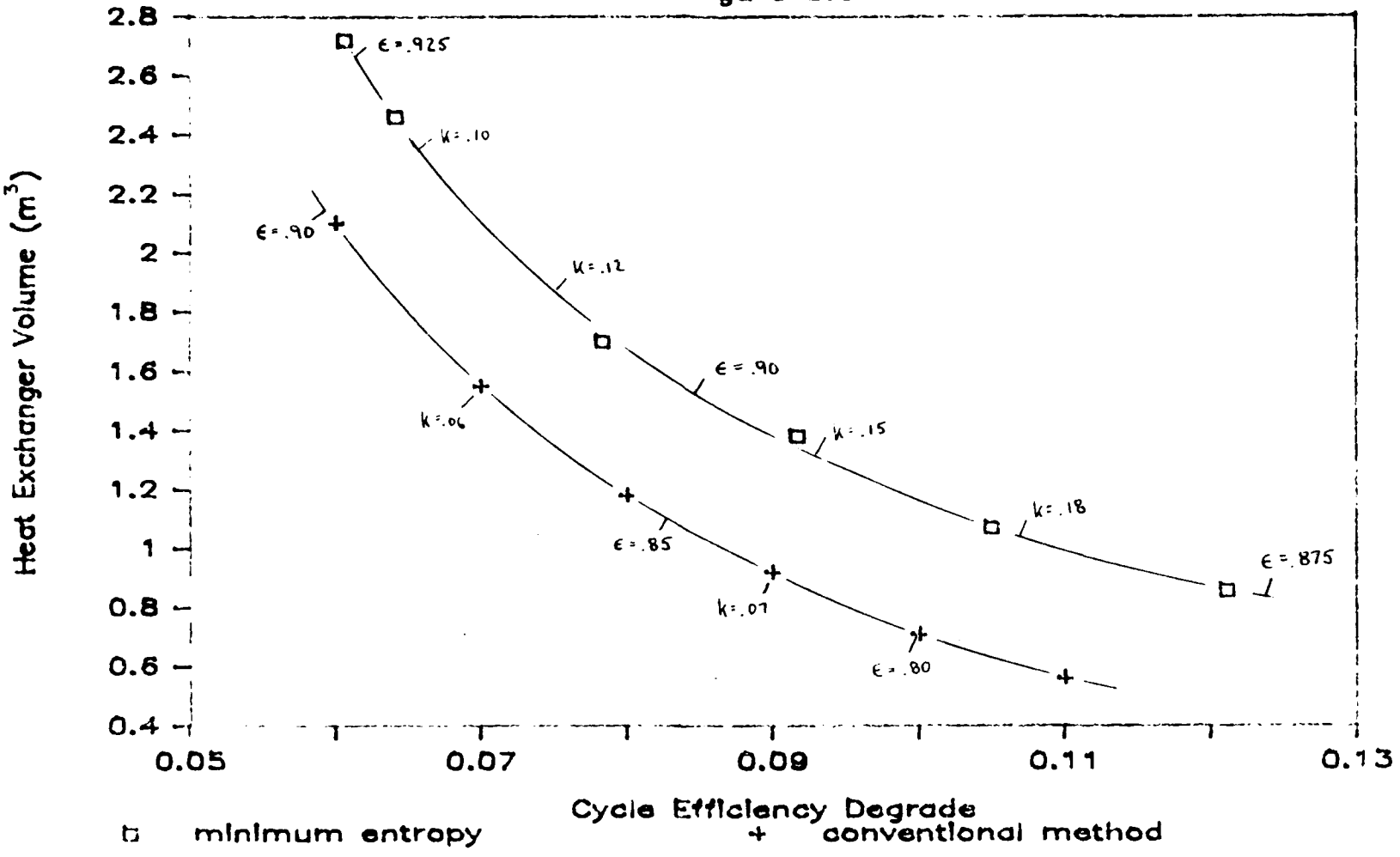

Chapter 6

CONCLUSIONS

6.1 Discussion

The nature of the results and conclusions drawn for the example cycle would be the same for other cycles and recuperator surfaces. For high effectiveness recuperators, the counterflow arrangement is dictated. Here with the same finned surface on both sides, the $(\Delta P/P)_c/(\Delta P/P)_h \simeq (P_h/P_c)^2$ or approximately 1/25. If a closer plate spacing were used on the clean air cold side more $\Delta P/P$ would appear on the cold side for any total $\Sigma P/P$. This would result in even smaller minimum volumes at any given N_s or $\eta_\infty - \eta$.

6.2 Conclusions

In selecting a gas turbine recuperator, essentially the same results are obtained either by the conventional method of minimizing degradation of cycle efficiency, $\eta_\infty - \eta$, or by minimizing entropy generation, N_s.

The selection of an "optimum" recuperator requires that care be exercised in the selection of the path along which the optimization is calculated. It has been shown that the volume of the recuperator for minimum N_s or $\eta_\infty - \eta$ along a constant mass velocity path is much greater than the true minimum volume at any $\eta_\infty - \eta$ or N_s.

Appendix A

Sample Calculation for Effect of Recuperator on Cycle Efficiency

$$\epsilon = 0.8,\ r = \frac{1}{6}$$

$$\eta_\infty = \frac{\dot{w}_{net}}{\dot{Q}} = \frac{\dot{w}_t + \dot{w}_c}{\dot{Q}}$$

$$\dot{w}_t = \dot{m}(h_4 - h_5) = \dot{m}c_p(T_4 - T_5)$$

$$\dot{w}_c = \dot{m}(h_1 - h_2) = \dot{m}c_p(T_1 - T_2)$$

$$\dot{Q} = \dot{m}(h_4 - h_3) = \dot{m}c_p(T_4 - T_3)$$

Turbine:

$$\frac{T_4}{T_5} = \left(\frac{P_4}{P_5}\right)^{(\eta_{pt})\left(\frac{\gamma-1}{\gamma}\right)}$$

$$T_5 = \left[\frac{\left(\frac{P_4}{P_5}\right)^{(\eta_{pt})\left(\frac{\gamma-1}{\gamma}\right)}}{T_4}\right]^{-1}$$

$$T_5 = \left[\frac{(6)^{(.9)(\frac{1.4-1}{1.4})}}{1300}\right]^{-1} = 820.1°k$$

Compressor:

$$\frac{T_2}{T_1} = \left(\frac{P_2}{P_1}\right)^{\frac{\gamma-1}{(\eta_{pc})(\gamma)}}$$

$$T_2 = T_1\left(\frac{P_2}{P_1}\right)^{\frac{\gamma-1}{(\eta_{pc})(\gamma)}}$$

$$T_2 = (300)(6)^{\frac{1.4-1}{(.95)(1.4)}} = 514.2°k$$

Recuperator:

$$\epsilon = \frac{T_3 - T_2}{T_5 - T_2}$$

$$T_3 = (\epsilon)(T_5 - T_2) + T_2$$

$$T_3 = (.8)(820.1 - 514.2) + 514.2 = 695.2°k$$

Cycle Efficiency:

$$\eta_\infty = \frac{(T_4 - T_5) + (T_1 - T_2)}{T_4 - T_3} = \frac{(1300 - 820.1) + (300 - 514.2)}{1300 - 695.2} = 0.4651$$

Appendix B

Conventional Design Method Numerical Example

Before calculations can be performed, two points need to be clarified: 1) the method of determining how loss of turbine work due to pressure drops in the system is distributed and; 2) the method for determining which side of the heat exchanger has the more stringent $\Delta P/P$ requirement.

Turbine work is given by the expression

$$\dot{w}_t = \dot{m}\eta_t c_p T_h \left[1 - \left(\frac{P_c}{P_h}\right)^\gamma\right]$$

$$\frac{\dot{w}_t}{\dot{m}\eta_t c_p T_h} = 1 - \left(\frac{P_c + \Delta P_c}{P_h - \Delta P_h}\right)^\gamma = 1 - \left(\frac{P_c}{P_h}\right)^\gamma \left[\frac{1 + \frac{\Delta P_c}{P_c}}{1 - \frac{\Delta P_h}{P_h}}\right]^\gamma$$

Expanding the last term,

$$\frac{\dot{w}_t}{\dot{m}\eta_t c_p T_h} \simeq 1 - \left(\frac{P_c}{P_h}\right)^\gamma \left[1 + \frac{\Delta P_h}{P_h} + \frac{\Delta P_c}{P_c} + \cdots\right]^\gamma$$

$$\frac{\dot{w}_t}{\dot{m}\eta_t c_p T_h} \simeq 1 - \left(\frac{P_c}{P_h}\right)^\gamma \left[1 + \gamma\left(\frac{\Delta P_h}{P_h} + \frac{\Delta P_c}{P_c}\right) + \cdots\right]$$

so that loss of turbine work can be expressed as

$$\frac{\Delta\dot{w}}{\dot{m}\eta_t c_p T_h} \simeq -\gamma\left(\frac{P_c}{P_h}\right)^\gamma \left(\frac{\Delta P_h}{P_h} + \frac{\Delta P_c}{P_c}\right)$$

and it is clear from Figure B.1 that $\Sigma\frac{\Delta P}{P}$ determines the loss of turbine work irregardless of how it is distributed. Introducing the definitions $r \equiv \frac{P_h}{P_c}$

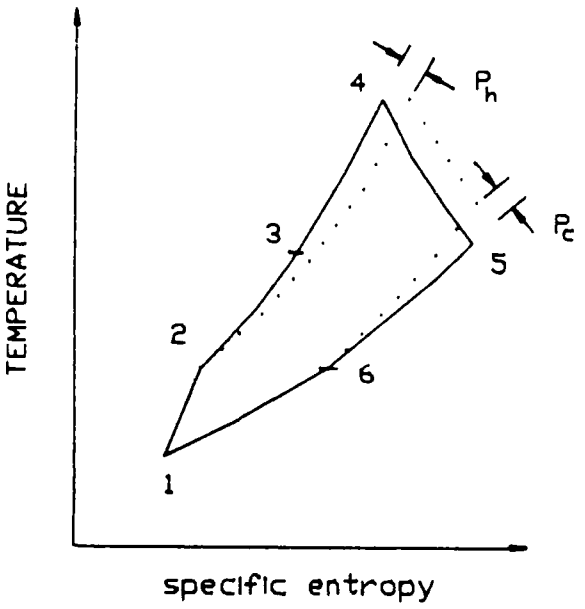

Temperature - Entropy Diagram
Figure B.1

and $\theta = \left(\frac{T_h}{T_c}\right)_{avg}$, it can be shown that for a counterflow exchanger where $A_c = A_h$ and $L_c = L_h$,

$$\frac{\Delta P_h/P_h}{\Delta P_c/P_c} = \frac{\theta}{r^2}$$

Using a slightly different form of the last turbine work expression,

$$\frac{\Delta \dot{w}_t}{\dot{m}\eta_t c_p T_h} = -\gamma \frac{1}{r^\gamma}\left[\frac{\Delta P_h/P_h}{\Delta P_c/P_c} + 1\right]\frac{\Delta P_c}{P_c}$$

$$\frac{\Delta \dot{w}_t}{\dot{m}\eta_t c_p T_h} = -\gamma \frac{1}{r^\gamma}\left(\frac{\theta}{r^2} + 1\right)\frac{\Delta P_c}{P_c}$$

$$\frac{\Delta \dot{w}_t}{\dot{w}_t} = -\gamma \frac{1}{r^\gamma} \frac{(\theta/r^2+1)}{(1-1/r^\gamma)} \frac{\Delta P_c}{P_c}$$

$$\frac{\Delta \dot{w}_t}{\dot{w}_t} = -\gamma \frac{(\theta/r^2+1)}{r^\gamma - 1} \frac{\Delta P_c}{P_c}$$

Introducing $\frac{\Delta P_c}{P_c} + \frac{\Delta P_h}{P_h} = k$, expressions for hot and cold side pressure drops are,

$$\frac{\Delta P_h}{P_h} = \frac{k(\theta/r^2)}{1+\theta/r^2}$$

$$\frac{\Delta P_c}{P_c} = \frac{k}{1+\theta/r^2}$$

The numbered steps that follow correspond to those outlined in Section 3.2. The input design parameters used for the example calculations were $\epsilon = 0.8$ and $k = 0.04$.

B.1 Temperatures and Fluid Properties

$$T_1 = 300°k$$

$$\frac{T_2}{T_1} = \left(\frac{P_2}{P_1}\right)^{\frac{\gamma-1}{\eta_{pc}\gamma}}$$

so that

$$T_2 = T_1 \left(\frac{P_2}{P_1}\right)^{\frac{\gamma-1}{\eta_{pc}\gamma}}$$

$$T_2 = 300(5)^{\frac{1.4-1}{(.95)(1.4)}} = 486.8°k$$

$$\frac{P_4}{P_5} = \frac{P_2}{P_1}(1-k) = 5(1-.04) = 4.8$$

$$\frac{T_4}{T_5} = \left(\frac{P_4}{P_5}\right)^{\eta_{pt}\left(\frac{\gamma-1}{\gamma}\right)}$$

$$T_5 = \left[\frac{\left(\frac{P_4}{P_5}\right)^{\eta_{pt}\left(\frac{\gamma-1}{\gamma}\right)}}{T_4}\right]^{-1}$$

$$T_5 = \left[\frac{(4.8)^{(.9)\left(\frac{1.4-1}{1.4}\right)}}{1300}\right]^{-1} = 868.5°k$$

$$\epsilon = \frac{T_3 - T_2}{T_5 - T_2}$$

so that

$$T_3 = \epsilon(T_5 - T_2) + T_2$$

$$T_3 = (.8)(868.5 - 486.8) = 792.2°k$$

Similarly

$$T_6 = T_5 - \epsilon(T_5 - T_2)$$

$$T_6 = 868.5 - (.8)(868.5 - 486.8) = 563.1°k$$

Since this is a counterflow design with $C^* > 0.5$, the best choice for average temperatures is the arithmetic average on each side

$$T_{hm} = \frac{T_5 + T_6}{2} = \frac{868.5 + 563.1}{2} = 715.8°k$$

$$T_{cm} = \frac{T_2 + T_3}{2} = \frac{486.8 + 792.2}{2} = 639.5°k$$

Inlet, outlet and average densities are next computed. $Pv = RT$ or $v = RT/P$ but $v = 1/\rho$, so $\rho = P/RT$

$$\rho_5 = \frac{1.126 \times 10^5 N/m^2}{(287 j/kg -° k)(868.5°k)} = 0.4517 kg/m^3$$

$$\rho_6 = \frac{1.126 \times 10^5}{(287)(563.1)} = 0.6967 kg/m^3$$

$$\left(\frac{1}{\rho}\right)_{m,h} = \frac{1}{2}\left(\frac{1}{\rho_5} + \frac{1}{\rho_6}\right) = 1.824 m^3/kg$$

$$\rho_2 = \frac{5.63 \times 10^5}{(287)(486.8)} = 4.030 kg/m^3$$

$$\rho_3 = \frac{5.63 \times 10^5}{(287)(792.2)} = 2.476 kg/m^3$$

$$\left(\frac{1}{\rho}\right)_{m,c} = 0.3260 m^3/kg$$

B.2 N_{tu}

For a couterflow heat exchanger,

$$\epsilon = \frac{1 - exp[-N_{tu}(1 - c^*)]}{1 - c^* exp[-N_{tu}(1 - c^*)]}$$

but for the balanced flow case ($c^* = 1$) under design,

$$\epsilon = \frac{N_{tu}}{1 + N_{tu}}$$

or

$$N_{tu} = \frac{\epsilon}{1 - \epsilon} = \frac{0.8}{1 - 0.8} = 4$$

Since gas is the working fluid on both sides, it was estimated that both sides would have approximately the same surface resistance so that

$$N_{tu,h} = N_{tu,c} \simeq 2N_{tu} = 8$$

B.3 Estimated Pressure Drops

Recall

$$\theta = \left(\frac{T_h}{T_c}\right)_{avg} = \frac{715.8}{639.5} = 1.1193$$

and

$$\frac{\theta}{r^2} = \frac{1.1193}{(1/5)^2} = 27.983$$

$$\frac{\Delta P_h}{P_h} = \frac{k(\theta/r^2)}{1+\theta/r^2} = \frac{(0.04)(27.983)}{1+27.983} = 0.03862$$

$$\frac{\Delta P_c}{P_c} = \frac{k}{1+\theta/r^2} = \frac{0.04}{1+27.983} = 0.00138$$

From Figure 2.3, an estimate of $j/f = 0.0035/0.0077$ was obtained.

B.4 Mass Velocities

The mass velocity on each side is estimated from the relationship

$$G = \left[\left(\frac{2g_c P \eta_o}{(1/\rho)_m N_{Pr}^{\frac{2}{3}}}\right)\left(\frac{\Delta P/P}{N_{tu}}\right)_{side}\frac{j}{f}\right]^{\frac{1}{2}}$$

As a first approximation, η_o was assumed to be 0.90.

$$G_h = \left[\left(\frac{(2)(1.126\times 10^5 N/m^2)(0.9)}{(1.824 m^3/kg)(0.7)^{\frac{2}{3}}}\right)\left(\frac{0.03862}{8}\right)\left(\frac{0.0035}{0.0077}\right)\right]^{\frac{1}{2}}$$

$$G_h = 17.586 kg/m^2 - s$$

$$G_c = \left[\left(\frac{(2)(5.63\times 10^5)(0.9)}{(.3260)(0.7)^{\frac{2}{3}}}\right)\left(\frac{0.00138}{8}\right)\left(\frac{0.0035}{0.0077}\right)\right]^{\frac{1}{2}}$$

$$G_c = 17.583 kg/m^2 - s$$

$$N_{Re,h} = \frac{G_h D_h}{\mu_h} = \frac{(17.583 kg/m^2 - s)(0.0474 ft)(.3048 m/ft)}{3.396\times 10^{-5} kg/m - s}$$

$$N_{Re,h} = 7481$$

$$N_{Re,c} = \frac{(17.583)(.0474)(.3048)}{3.159 \times 10^{-5}} = 8042$$

Entering Figure 2.3 with these values yields

$$f_h = 0.0078$$

$$j_h = 0.00355$$

$$f_c = 0.0077$$

$$j_c = 0.0035$$

B.5 Heat Transfer Coefficients and Fin Effectivenesses

With the Colburn factor known, the heat transfer coefficient can be determined from

$$h = jGc_p P_r^{-\frac{2}{3}}$$

This result is used to compute the fin characteristic length,

$$m = \left(\frac{2h}{k_f \delta}\right)^{\frac{1}{2}}$$

The temperature effectiveness of the fin is next calculated from

$$\eta_f = \frac{tanhml}{ml}$$

A good approximation for l is given by half the plate spacing minus the fin thickness.

The total surface temperature effectiveness can then be calculated

$$\eta_o = 1 - (1 - \eta_f)A_f/A$$

where A_f/A is a characteristic of the surface selected.

$$h_h = \frac{(0.00355)(17.586kg/m^2 - s)(1.0kj/kg - ^\circ k)}{(0.7)^{\frac{2}{3}}}$$

$$h_h = 79.19 w/m^2 -^\circ k$$

$$m_h = \left[\frac{(2)(79.19 w/m^2 -^\circ k)}{(190 w/m -^\circ k)(0.032 in)(0.0254 m/in)}\right]^{\frac{1}{2}}$$

$$m_h = 32.024 m^{-1}$$

$$l = \left(\frac{0.750}{2} in - .032 in\right) 0.0254 m/in$$

$$l = 8.71 \times 10^{-3} m$$

$$\eta_{f,h} = \frac{tanh(32.024)(0.71 \times 10^{-3})}{(32.024)(0.71 \times 10^{-3})}$$

$$\eta_{f,h} = 0.9749$$

$$\eta_{o,h} = 1 - (1 - 0.9749)(.606)$$

$$\eta_{o,h} = 0.9848$$

$$h_c = \frac{(0.00355)(17.583)(1.0)}{(0.7)^{\frac{2}{3}}} = 78.06 w/m^2 -^\circ k$$

$$m_c = \left[\frac{(2)(78.06)}{(190)(0.032)(0.0254)}\right]^{\frac{1}{2}} = 31.79 m^{-1}$$

$$\eta_{f,c} = \frac{tanh(31.79)(8.71 \times 10^{-3})}{(31.79)(8.71 \times 10^{-3})} = 0.9752$$

$$\eta_{o,c} = 1 - (1 - .9752)(.606) = 0.9850$$

The overall heat transfer coefficient can now be determined neglecting foul-

ing resistances and wall thermal resistances,

$$\frac{1}{U} = \frac{1}{(\eta_o h)_h} + \frac{1}{(\eta_o h)_c}$$

$$\frac{1}{U} = \frac{1}{(0.9848)(79.19)} + \frac{1}{(.9850)(78.06)} = 0.02583$$

$$U = 38.714 w/m^2 - ^\circ k$$

B.6 Dimensions

The heat transfer surface area is computed from

$$A = \frac{N_{tu} C}{U}$$

$$A = \frac{(4)(3600 kg/hr)(1.0 kj/kg - ^\circ k)}{38.714 w/m^2 - ^\circ k} = 103.32 m^2$$

Minimum free flow area is given by

$$A_o = (W/G) = \frac{3600 kg/hr}{17.586 kg/m^2 - s} = 0.05686 m^2$$

In order to determine frontal area, σ must be computed from the relationship

$$\sigma = \frac{d \beta D_h / 4}{d + d + 2t}$$

Here a parting plate thickness of $0.4mm$ was assumed, so

$$\sigma = \frac{(0.75in)(76.1 ft^2/ft3)(0.0474/4ft)}{0.75in + 0.75in + 2(.4mm)(.1/2.54\ in/mm)}$$

$$\sigma = 0.44162$$

$$A_{fr} = A_o/\sigma$$

$$A_{fr} = \frac{0.05686 m^2}{0.44162} = 0.12876 m^2$$

The flow length is given by

$$L = \left(\frac{D_h A}{4A_o}\right)$$

$$L = \frac{(0.0474ft)(0.3048m/ft)(103.321m^2)}{(4)(0.05686m^2)}$$

$$L = 6.56m$$

The total volume of the heat exchanger is calculated by

$$Vol = (A_{fr})(L)$$

$$Vol = (0.12876m^2)(6.56m) = 0.845m^3$$

B.7 Calculated Pressure Drops

For this level of design, entrance and exit effects are not considered, so only core friction effects will be used.

$$\frac{\Delta P}{P} = f(L/r_h)(1/\rho)_m G^2/2P$$

$$\frac{\Delta P_h}{P_h} = \frac{(0.0078)(6.56)(1.824)(17.586)^2}{(2)(0.0474/4)(.3048)(5.63 \times 10^5)} = 0.00125$$

Similarly

$$\frac{\Delta P_c}{P_c} = 0.00125$$

so that

$$\Sigma \frac{\Delta P}{P} = 0.03674$$

The cycle efficiency with these input parameters is

$$\eta = \frac{(T_4 - T_5) + (T_1 - T_2)}{T_4 - T_3}$$

$$\eta = \frac{(1300 - 868.5) + (300 - 486.8)}{(1300 - 792.2)}$$

$$\eta = 0.4819$$

and the efficiency degrade is given by $\eta_\infty - \eta$.

$$\eta_\infty - \eta = 0.5760 - 0.4819 = 0.0941$$

Appendix C

Minimum Entropy Design Method Numerical Example

This example uses the data from case C-12 of Table 3.1, $G = 12.456 kg/m^2 - s$, $j = 0.00355$, and $f = 0.0078$.

C.1 Optimum Length

In order to use equation (4.24), intermediate values must first be determined

$$N_{st} = \frac{j}{(N_{pr})^{2/3}} = \frac{0.00355}{(0.7)^{2/3}} = 0.00450$$

The temperature span parameter, τ, cannot be calculated until T_5 is known, so an estimate based on previous iterations is used. If the calculated value of τ is close to the value used, the computations are valid.

$$(L/r_h)_{opt} = \frac{2}{G}\left(\frac{\tau/N_{st}}{Bf(1/\rho_c P_c + 1/\rho_h P_h)}\right)^{\frac{1}{2}}$$

$$(L/r_h)_{opt} = \frac{2}{12.456}\left(\frac{0.365/0.00450}{(0.287)(0.0078)\left(\frac{0.325}{5.63\times 10^5} + \frac{1.818}{1.126\times 10^5}\right)}\right)^{\frac{1}{2}}$$

$$(L/r_h)_{opt} = 5283$$

Since r_h is set by the geometry selected, L can be calculated

$$L_{opt} = 5283(.0474ft)(.3048m/ft)$$

$$L_{opt} = 19.08m$$

C.2 Heat Exchanger Effectiveness and Pressure Drops

From equation (4.16),

$$N_{tu,h} = (L/r_n)N_{st}$$

$$N_{tu,h} = (5283)(0.00450) = 23.79$$

Applying the same assumption as was used in Chapter 3,

$$N_{tu,h} = N_{tu,c} = 2N_{tu}$$

$$N_{tu} = 23.79/2 = 11.89$$

Then, since this is still a balanced counterflow design,

$$\epsilon = \frac{N_{tu}}{1+N_{tu}} = \frac{11.89}{1+11.89} = 0.922$$

For hot and cold side pressure drops, equation (4.17) is used.

$$(\frac{\Delta P}{P})_h = f(L/r_h)g^2/(2\rho P) = f(L/r_h)g^2$$

$$(\frac{\Delta P}{P})_h = (0.0078)(5283)(0.05005)^2 = 0.010322$$

$$(\frac{\Delta P}{P})_c = (0.0077)(5283)(0.00946)^2 = 0.00369$$

$$\Sigma\frac{\Delta P}{P} = 0.10322 + 0.00369 = 0.1069$$

C.3 Entropy Generation

Equations (4.14) and (4.15) will be used to determine entropy generation on both sides.

$$Ns_h = \frac{\tau^2}{N_{tu,h}} + \left(\frac{R}{c_p}\right)_h \left(\frac{\Delta P}{P}\right)_h$$

$$Ns_h = \frac{0.365}{23.79} + (0.287)(0.10322)$$

$$Ns_h = 0.04497$$

$$Ns_c = \frac{0.365}{23.79} + (0.287)(0.00369)$$

$$Ns_c = 0.0164$$

$$Ns = Ns_h + Ns_c$$

$$Ns = 0.04497 + 0.0164 = 0.0614$$

C.4 Heat Exchanger Volume

Since A_{fr} is calculated from minimum free flow area and other surface geometrical constraints,A_{fr} from the corresponding case in Chapter 3 was used to calculate the heat exchanger volume.

$$Vol = L(A_{fr}) = 19.08m(0.12876m^2) = 2.46m^3$$

C.5 Cycle Efficiency Degrade

Temperatures that reflect the actual effectiveness and pressure drop must first be determined.

$$\frac{P_4}{P_5} = \frac{P_2}{P_1}(1-k) = 5(1-0.1069) = 4.465$$

$$T_5 = \left[\frac{\left(\frac{P_4}{P_5}\right)^{\eta_{pt}\left(\frac{\gamma-1}{\gamma}\right)}}{T_4} \right]^{-1}$$

$$T_5 = \left[\frac{(4.465)^{\frac{(.9)(1.4-1)}{1.4}}}{1300} \right]^{-1} = 884.8^\circ k$$

$$T_3 = \epsilon(T_5 - T_2) + T_2$$

$$T_3 = 0.922(884.8 - 486.8) + 486.8$$

$$T_3 = 853.8^\circ k$$

$$\eta = \frac{(T_4 - T_5) + (T_1 - T_2)}{T_4 - T_3}$$

$$\eta = \frac{(1300 - 884.8) + (300 - 486.8)}{1300 - 853.8} = 0.5119$$

$$\eta_\infty - \eta = 0.5760 - 0.5119 = 0.06412$$

A check on the validity of the τ value assumed shows

$$\tau = \left(\sqrt{\frac{T_5}{T_2}} - \sqrt{\frac{T_2}{T_5}} \right)^2$$

$$\tau = \left(\sqrt{\frac{884.8}{486.8}} - \sqrt{\frac{486.8}{884.8}} \right)^2$$

$$\tau = 0.367$$

Therefore, assumed value of 0.365 was valid

Appendix D

Sample Calculation of Entropy Generation for Conventional Designs

Example uses case C-12. From previous example,

$$\tau = 0.34461$$

$$\frac{\Delta P_h}{P_h} = 0.0359$$

$$\frac{\Delta P_c}{P_c} = 0.00136$$

$$N_{tu,h} = N_{tu,c} = 8$$

Using equations (4.14) and (4.15),

$$N_{s,h} = \frac{\tau}{N_{tu,h}} + \left(\frac{R}{C_p}\right)_h \left(\frac{\Delta P}{P}\right)_h$$

$$N_{s,h} = \frac{0.34461}{8} + (0.287)(0.0359) = 0.05338$$

Similarly,

$$N_{s,c} = \frac{0.34461}{8} + (0.287)(0.00136) = 0.04347$$

$$N_s = N_{s,h} + N_{s,c} = 0.09685$$

Adding the first term of each side's expression gives the ΔT contribution, and the sum of the second terms is the ΔP contribution to the entropy generation.

$$N_{s,\Delta T} = 0.08615$$

$$N_{s,\Delta P} = 0.01070$$

Bibliography

[1] Bejan, A., *"Second Law Analysis in Heat Transfer,"* Energy, Vol.5, 1980, p.721.

[2] Kakac, Bergles and Mayinger, Heat Exchangers-Thermohydraulic Fundamentals and Design, Hemisphere Publishing Corp., Washington, D.C., 1981.

[3] Bejan, A., *"A Study of Entropy Generation in Fundamental Convective Heat Transfer,"* Transactions of the ASME, Vol. 101, November 1979, p.718.

[4] Bejan, A. *The Concept of Irreversibility in Heat Exchanger Design: Counterflow Heat Exchangers for Gas-to-Gas Applications,"* Transactions of the ASME, Vol. 99, August 1977, p.374.

[5] Kays, W. and London, A., Compact Heat Exchangers, McGraw-Hill, New York, 1964.

[6] Bejan, A., Entropy Generation Through Heat and Fluid Flow, Wiley, New York, 1982.

END

DATE

FILMED

4-88

DTIC